FACULTY OF MEDICINE AND HEALTH SCIENCES

An animal model for transvascular optogenetics

Word count: 18,279

De Wilde Maaike
Student number: 01305516

Supervisor(s): Dr. Vincent Keereman, Prof. dr. Robrecht Raedt

A dissertation submitted to Ghent University in partial fulfilment of the requirements for the degree of Master of Science in the Biomedical Sciences

Academic year: 2017 - 2018

GHENT UNIVERSITY

FACULTY OF MEDICINE AND HEALTH SCIENCES

An animal model for transvascular optogenetics

Word count: 18,279

De Wilde Maaike
Student number: 01305516

Supervisor(s): Dr. Vincent Keereman, Prof. dr. Robrecht Raedt

A dissertation submitted to Ghent University in partial fulfilment of the requirements for the degree of Master of Science in the Biomedical Sciences

Academic year: 2017 - 2018

GHENT UNIVERSITY

PREFACE

Both writing this dissertation and performing experiments in the Laboratory for Clinical and Experimental Neurophysiology, Neurobiology and Neuropsychology were a very educational experience. After a year of hard work, this thesis was realized, also thanks to the help and support of many people. I would like to take this opportunity to thank these people.

First of all I would like to thank my promotor Dr. Vincent Keereman for his help to define the research questions and input during interim discussions. I also would like to thank my copromotor Prof. Dr. Robrecht Raedt to supervise me during my practical work and for the feedback and help during discussions.

In addition, there was no question too much for the PhD students. On top of this, they learned me some techniques and helped if necessary. Thanks, Anirudh, Charlotte B., Charlotte G., Jana, Latoya, Marie and Wouter. Latoya deserves an extra thank you for proofread this thesis. I would also like to thank the other Master's students, Caroline, Dinah, Erine and Gilles, for their support and help. It was nice to work with you!

Finally, I would also like to thank my parents for their endless support and for giving me the opportunity to start this education in Biomedical sciences and bring it to a successful end.

TABLE OF CONTENTS

SAMENVATTING

Achtergrond: Epilepsie wordt gekarakteriseerd door epileptische aanvallen uitgelokt door een hypersynchrone neuronale activiteit in een hyperexciteerbaar neuronaal netwerk. Actuele behandelingen, zoals anti-epileptica, resectieve chirurgie en neurostimulatie, hebben niet altijd het gewenste effect. Optogenetica kan een nieuwe therapie zijn omdat het neuronale activiteit celspecifiek en spatiotemporeel onder controle kan houden. Desondanks blijkt zijn invasieve karakter een hindernis.

Methoden: De mogelijkheid tot transvasculaire optogenetische modulatie bij de rat werd onderzocht door optische stimulatie van neuronen die channelrhodopsine-2 (ChR2) en Guillardia theta anion channelrhodopsine-2 (GtACR2) tot expressie brengen in de cortex, met blauw licht afkomstig van een optische vezel geplaatst in de sinus sagittalis superior (SSS). De optimale stimulatieparameters, namelijk benodigd vermogen, pulsduur en stimulatiefrequentie, maar ook de maximale afstand tot waar modulatie nog mogelijk is werden bepaald.

Resultaten: Transvasculaire optogenetische modulatie van neuronen die ChR2 en GtACR2 tot expressie brengen is respectievelijk mogelijk tot 1.5-2.5mm en 1.9-2.1mm onder de dura mater en een afstand van 0.9-1.3mm en 0.6-0.9mm lateraal van de wand van de SSS. Hiervoor was een vermogen van 2.3mW noodzakelijk. De amplitude van de geëvokeerde potentialen (EP) stijgt met een toenemend vermogen bij pulsen van 1ms, 3ms, 10ms en 25ms. Deze pulsduren blijken optimaal voor transvasculaire optogenetische stimulatie. Lagere frequenties attenueren EP minder bij beide opsines en zijn dus de meest optimale stimulatiefrequenties.

Besluiten: Deze studie gaf een eerste indruk over transvasculaire optogenetische stimulatie en zijn optimale stimulatieparameters, maar verder onderzoek is noodzakelijk om deze te bevestigen en de mogelijke anti-epileptische effecten van neuronale inhibitie met GtACR2 verder te onderzoeken.

SUMMARY

Background: Epilepsy is characterized by epileptic seizures due to a hypersynchronous neuronal activity in a hyperexcitable neuronal network. Current treatments such as anti-epileptic drugs, resective surgery and neurostimulation do not always have the desired effect. Optogenetics, which provides a spatiotemporal and cell-type specific control of neuronal activity, can be a solution. But a current hurdle is its invasive nature.

Methods: The possibility of transvascular optogenetic modulation in the rat was determined through optical stimulation of channelrhodopsin-2 (ChR2) and Guillardia theta anion channelrhodopsin-2 (GtACR2) expressing cortical neurons with blue light with an optic fiber placed into the sinus sagittalis superior (SSS). The optimal light stimulation parameters: required power, pulse duration and frequency and also the maximal distance at which modulation is still possible were determined.

Results: Transvascular optogenetic modulation of ChR2 and GtACR2 expressing neurons is respectively possible up to 1.5-2.5mm and 1.9-2.1mm under the dura mater and 0.9-1.3mm and 0.6-0.9mm lateral to the edge of the SSS. Therefore, a power of 2.3mW was required. The evoked potential (EP) amplitude rises with an increasing output power at 1ms, 3ms, 10ms and 25ms pulses. These pulse durations are optimal for transvascular stimulation. Lower frequencies caused less attenuation of EP amplitude, with both opsins, and are thus the most optimal stimulation frequencies.

Conclusions: This study gave a first impression of transvascular optogenetic stimulation and its optimal stimulation parameters, but further research is necessary to confirm these parameters and investigate the possible anti-epileptic effects of neuronal inhibition with GtACR2.

1 INTRODUCTION

1.1 EPILEPSY

Epilepsy is a chronic neurological disorder characterized by repeated and spontaneous epileptic seizures which affects 65 million people or roughly one percent of the population worldwide [1-3]. These epileptic seizures are due to a hypersynchronous neuronal activity in a hyperexcitable neuronal network in the brain, spreading to an increasing number of neurons in that neuronal network [1, 4-7]. Disturbances of behaviour and consciousness occur during these seizures, e.g. staring and small shocks of the limbs. During the well-known tonic-clonic seizures, the tonic phase is characterized by stiffening of the body followed by shocks of the limbs during the clonic phase [1, 8]. The severity of symptoms during seizures depends on the localisation, extent, spread and intensity of the neurophysiological electrical disorder of the brain. A distinction can be made between generalized epileptic seizures, for example absence seizures, and partial epileptic seizures [4, 8]. Epilepsy can be caused by trauma, infections, tumours or can have genetic reasons [9, 10]. This is due to an imbalance between the excitatory glutamatergic system and inhibitory gamma-aminobutyric acid (GABAergic) system induced by these different causes [11, 12]. Epilepsy is associated with a loss of GABAergic interneurons which leads to an impaired inhibition of principal neurons. Mossy fiber sprouting is associated with temporal lobe epilepsy (TLE) which implies that it also strengthens the excitatory glutamatergic neurons. Both the impaired inhibition and excitatory strengthening reinforce the imbalance and this may lead to a greater network hyperexcitability [12].

About seventy percent of the epileptic patients can be treated with anti-epileptic drugs (AEDs) [1], such as GABA receptor agonists, neurotransmitter receptor agonists and sodium channel blockers [13], but in approximately thirty percent of the patients, epilepsy cannot be controlled with these AEDs, or adverse side-effects, e.g. drowsiness and decrease in cognitive functions, are too severe [2]. This is called refractory epilepsy [14]. AEDs are furthermore acting on multiple targets, affecting surrounding cells and normal brain function [15, 16]. Surgical removal of the epileptic focus, which is the region in the brain that causes epileptic seizures [1], can be a solution. This is called resective surgery [3]. However, this surgery is not always possible because of the localisation of the epileptic focus. If the epileptic focus overlaps with functionally essential brain tissue, for example the motor cortex or speech-related brain areas, the epileptic focus cannot be removed with surgery. Because of this, it is very important to exactly localize the epileptic focus [1]. Disconnection surgery can be a second solution [3]. Although surgery has the best outcome in the field of seizure freedom, it is also associated

with risks and is not always successful. Another alternative treatment is neurostimulation, namely deep brain stimulation, transcranial magnetic stimulation and vagus nerve stimulation, which allows for a more targeted therapy compared to AEDs and surgery. Moreover, it allows for a temporally precise stimulation of neurons and overcomes the irreversibility of surgery [5, 7]. But neurostimulation is not hundred percent effective and can still result in adverse side-effects because electrical stimulation is not cell-type specific [3, 5, 7, 15, 16]. Because of the limited success, adverse side-effects and high costs of the above-mentioned epilepsy treatments, it is necessary to develop new anti-epileptic therapies [17]. One of them is optogenetics, which provides a spatiotemporal and cell-type specific control of neuronal activity with light and opsins, which are light-sensitive ion channels and pumps [2, 5, 18-20]. Optogenetics does also not generate stimulation artefacts in contrast with electrical stimulation [7]. Because of the more precise mechanism of action compared to all the above-mentioned therapies, optogenetics may be more effective and minimize the adverse side-effects [15].

Another new anti-epileptic therapy that is being investigated is chemogenetics. Like optogenetics, chemogenetics also enables cell-type specific control of neuronal activity [21]. This technique uses engineered ligand gated ion channels and designer receptors exclusively activated by designer drugs (DREADDs), which are genetically modified G-protein coupled receptors. These DREADDs are no longer activated by endogenous neurotransmitters such as acetylcholine, but only via inert designer drugs such as clozapine N-oxide (CNO). Delivery of CNO results in neuronal silencing or excitation depending on the DREADDs within minutes to hours. In contrast with optogenetics, chemogenetics does not provide a fast temporal control of neuronal activity and on top of this, the pattern of activation can also not be controlled [11, 21, 22].

1.2 OPTOGENETICS

Optogenetics is a technology, which can control neuronal activity with light, that was discovered 10 years ago [2, 23]. With this technique, opsins are delivered into the brain. As a result, neurons in the brain are genetically manipulated and become sensitive to light of a specific wavelength through expression of these opsins [2, 24]. Subsequently, the target area can be reached with light of a specific wavelength through an optic fiber and specific neurons can be excited/inhibited by illumination with a high spatiotemporal resolution [2, 24]. This technique will be further discussed in more detail in sections 1.2.1-1.2.7. These sections will handle different methods of genetic delivery, with a whole description of an adeno-associated

viral vector (AAV), optic fibers, methods of light delivery and different important stimulation parameters.

Optogenetics can be used in different biological systems ranging from cultured neurons to freely moving animals [2]. On top of this, it has already been shown to be effective at treating seizures in animal models of epilepsy if the location of the epileptic focus is known [2, 12]. Treatment of epilepsy relies on reversible selective inhibition of synaptic excitation, which involves inhibiting pyramidal neurons and increasing synaptic inhibition with inhibitory opsins selectively expressed in these pyramidal neurons. It also relies on reversible selective excitation of inhibitory interneurons with excitatory opsins selectively expressed in these interneurons, allowing a normalisation of excitability and stopping of epileptic seizure generation [6, 12, 24]. Because of this, optogenetics has recently gained more prominence as a potential therapy in (refractory) epileptic patients [25]. Besides the treatment of epilepsy, optogenetics had already been used to investigate the capacities to treat motor deficits in Parkinson's Disease and as well in Alzheimer's Disease [24]. Network interactions and the role of specific populations of neurons in the mechanisms of various brain functions had also been explored using optogenetics [12, 20]. Network excitability can also be regulated by this technology allowing for therapeutic interventions in brain diseases [12]. Other applications for optogenetics are for example: regulation of neurophysiological processes related to the dopaminergic system, treating narcolepsy and depression, fighting obesity, studying neural mechanisms of memory and regulation of sleep [23].

1.2.1 Methods of genetic delivery

With optogenetics, opsins need to be delivered into neurons. This requires genetic manipulation. Therefore, transgenic animals or transfection techniques such as viral vectors and *in utero* electroporation can be used [2, 12, 16]. Viral vectors, namely retroviruses/lentiviruses and AAVs, are the most commonly used transduction techniques and can be used from rodents to primates to target opsin gene expression [2, 16, 26]. On top of this, viral vectors can be easily delivered directly into specific brain regions limiting tissue damage. Viral vector delivery is also associated with a robust transduction efficacy [20].

Both lentiviruses and AAVs have a long-term stable transgene expression of several months [2, 12, 16]. High levels of functional opsin gene expression are seen during this period [16]. Furthermore, lentiviruses and AAVs can be easily produced within a few weeks in Biosafety Level 2 facilities [16]. AAVs provide a more effective and greater spatial spread when injected and expressed into the cortex in contrast with lentiviruses [20]. Unlike *in utero* electroporation,

which can be used to deliver transgenes of any size [16], the same disadvantage presents itself by using lentiviruses and AAVs. These viral vectors are small and have a limited genetic load, which consists of a transgene and promotor [2]. The limited genetic load is 4.7-4.9kb for AAVs and 10kb for lentiviruses [2, 12]. Because of this, these vectors are often incompatible for the full promotor, which affects the specificity of expression [2, 12]. Cell-type selectivity can also be obtained using Cre-dependent expression of the opsin [20]. Lentiviruses preferentially transduce excitatory neurons, thus an AAV is more suitable for transduction to target inhibitory interneurons [20].

In contrast to lentiviruses, which are natural pathogens that can transcribe themselves into the host genome of non-dividing cells, the non-immunogenic AAV can only transduce non-dividing cells without transcribing them in the host genome [12]. Because of their safety [5], AAVs are the most commonly used viral vectors [12]. A typical AAV is constructed with a promotor, opsin and reporter [2]. This will be further discussed in sections 1.2.2, 1.2.3 and 1.2.4. Several different AAV serotypes are available. These serotypes each have a different tropism, which means that they each preferentially target specific cell types within the host. The serotypes 1, 2, 5, 8 and 9 are shown to be effective to tranduce neurons in the brain, but they each have a different distribution and transduction efficiency [16].

1.2.2 Opsins

Opsins are light sensitive transmembrane proteins that translocate ions across the cell membrane when exposed to light of a specific wavelength. The effect on the membrane potential depends on the type of opsin (ion channel or pump [23, 27]), type of ions and their direction of movement. These ions can either excite/depolarize or inhibit/hyperpolarize neurons [2, 12, 28]. Type 1 microbial opsins, which are present in bacteria, archeabacteria and unicellular algae, are mainly used in optogenetics [2, 29]. Ion pumps generate much smaller currents, because they translocate only one charge per absorbed photon across the membrane [23, 27, 30]. This makes them less efficient than ion channels, which allow influx of many ions because they remain open for some time after light absorption [28, 30].

1.2.2.1 Excitatory opsins

1.2.2.1.1 Channelrhodopsin-2 (ChR2)

ChR2 is a non-selective cation channel from *Chlamydomonas reinhardtii* (green flagellate algae [27]), sensitive to blue light with a wavelength of 470nm [2, 12]. If ChR2 is exposed to blue light, ChR2 undergoes a conformational change from all-trans-retinal to 13-cis-retinal. Because of this, the pore of the transmembrane protein is opened and there is a passive

movement of Na^+, H^+, Ca^{2+} and K^+ ions. These ions depolarize the cell membrane and action potentials (AP) are generated within 50ms after illumination with blue light [6, 12, 26, 31]. ChR2 allow to safely, precisely and reversibly activate neurons in response to blue light [5, 31].The intensity of a LASER beam on a surface is stated as mW/mm^2. A minimal blue light intensity of $1mW/mm^2$ is required for generation of ChR2 evoked AP. Robust spiking is achieved with a blue light intensity of $10mW/mm^2$ [18]. Excitatory pyramidal neurons in the cortex expressing ChR2 can fire reliable spike trains across a range of firing frequencies up to 30-50Hz [16, 19, 31, 32]. Brief pulses of light activate ChR2 and because of this, spike trains are provoked [31]. 13-cis-retinal relaxes back to all-trans-retinal within milliseconds. This event closes the pore of the transmembrane protein and stops the flow of cations. Because of the fast (in)activation kinetics of this opsin, specific groups of neurons can be precisely and selectively stimulated [12, 26]. The expression of ChR2 in neurons has no influence on the cell health, membrane integrity and electrical properties of the neurons, also not after light exposure [31].

Besides ChR2, also ChR2 modifications were developed, to improve expression and increase light sensitivity of ChR2 and alter spectral properties, conductance or kinetics. ChR2 modifications are for example: ChR2-H134R, ChIEF channel, ChETA and other red-shifted ChR variants [2, 12, 16]. The ChR2-H134R modification has enhanced cellular photocurrents but a slower deactivation kinetic [16]. The ChETA variant has a faster opening and closing rate, but with reduced photocurrents. This is in contrast with the ChIEF variant, which has a slower kinetic but an increased light sensivity [26].

1.2.2.1.2 Channelrhodopsin-1 (ChR1)

ChR1 is a light-gated selective proton channel from *Chlamydomonas reinhardtii* (green flagellate algae) [31, 33, 34]. A passive conductance of ions occur through these channels during light exposure after the channel is opened [34].

1.2.2.2 Inhibitory opsins

1.2.2.2.1 Halorhodopsin (NpHR)

NpHR is an inward chloride pump from halobacterium *Natronomonas pharaonic,* sensitive to yellow light with a wavelength of 570nm. NpHR actively pumps Cl^- ions into the cell with millisecond kinetics, hyperpolarizing neurons and inhibiting AP [2, 6, 12, 35]. NpHR can safely, precisely and reversibly inhibit neuronal activity when expressed in neurons with yellow light pulses [5, 35]. This opsin can be used to control hyperexcitability of neurons during epileptic seizures in specific brain regions [17].

1.2.2.2.2 Archeorhodopsin (Arch)

Arch is an outward proton pump from halobacterium *Halorubrum sodomense*, sensitive to orange-yellow light with a wavelength of 575nm. The efflux of protons is responsible for hyperpolarization of neurons and inhibition of AP firing [2, 12].

1.2.2.2.3 Guillardia theta anion channelrhodopsin-2 (GtACR2)

GtACR2 is an inward ion channel at the holding potential (E_h) of -60mV with a very high selectivity for Cl^- ions. GtACR2 originates from the cryptophyte algae *Guillardia theta* and is very sensitive to blue light with a wavelength of 470nm [23, 24, 27, 28, 30, 35]. High conductance, robust expression and a deactivation kinetics of >40ms are specific properties of GtACR2 channels [30, 36]. Large photocurrents reverse when the membrane potential shifts to more positive values [27, 30]. GtACR2 is not permeable for cations [27]. GtACR2 allow for a precise control of neuronal activity because of its fast inactivation kinetics [24, 28]. Spiking can be precisely suppressed in GtACR2 expressing neurons with a blue light intensity of 0.005mW/mm^2 at frequencies up to at least 25Hz [27]. Dolgikh et. al found that this inhibition have exact the same duration as the illumination with blue light [24].

Normally, the cytoplasmic Cl^- concentration and also the concentration of Cl^- in the soma is low in neurons. If GtACR2 is illuminated for a long time (>100ms) with blue light, it generates hyperpolarizing currents through an influx of Cl^- in the soma at E_h above the Nernst equilibrium potential for Cl^- [13, 27]. In this way, GtACR2 is a strong cell silencer [28]. In contrast to the soma, the Cl^- concentration in the axons is higher, which leads to a depolarisation and AP generation through an efflux of Cl^- ions upon short illumination (<100ms) [13, 28]. This makes GtACR2 also a cell activator on top of a cell silencer [28].

1.2.2.2.4 Guillardia theta anion channelrhodopsin-1 (GtACR1)

GtACR1 is an inward ion channel at the E_h of -60mV permeable for Cl^- ions, but not for cations. It has a maximum absorption peak at 515nm [23, 27, 36]. Like GtACR2, GtACR1 channels have also a high conductance and require low light intensities for activation [36]. Photocurrents reverse when the membrane potential shifts to more positive values [27]. Illumination of GtACR1 leads to a hyperpolarization through the influx of Cl^- ions if the Cl^- concentration is low, for example in the soma. This happens at membrane potentials above the Nernst equilibrium potential for Cl^- ions, which implicates that GtACR1 is only capable of passive transport of Cl^- ions. If the Cl^- concentration is higher, for example in the presynaptic terminals, photoexcitation of GtACR1 leads to stimulation rather than inhibition of synaptic release [23, 28].

1.2.3 Promotors

There are two types of promotors: cell-type specific promotors and ubiquitous promotors [2]. Cell-type specific promotors are for example promotors for α-calcium/calmodulin-dependent kinase II (CamKIIα), the calcium-binding protein parvalbumin, somastotatin and glutamic acid decarboxylase-67 (GAD67). Promotors for CamKIIα expresses opsins in the forebrain excitatory pyramidal neurons while promotors for parvalbumin, somastotatin and GAD67 target inhibitory neurons [2, 11, 12]. Examples of ubiquitous promotors are: promotors for elongation factor-1α and cytomegalovirus, that give robust opsin expression in almost any cell type. Furthermore, promotors for synapsin are ubiquitous promotors that only target neurons [2].

1.2.4 Reporters

Reporters are genetically encoded fluorescence proteins, for example: green fluorescent protein (GFP), enhanced yellow fluorescent protein (eYFP) and mCherry [2]. In AAV, reporters are coupled to the opsin. Reporters make it possible to visualize and verify opsin expression.

1.2.5 Optic fibers

Optic fibers are light guides used to illuminate deep brain areas when coupled to a Light Amplification by Stimulated Emission of Radiation (LASER) or light emitting diode (LED) system with a patch cord [2, 29]. The light spreads out of the optic fiber tip as a cone [20]. Light intensity delivered to tissue varies with the numerical aperture (NA) and radius of the optic fiber and with the distance from the light source [3, 20]. It is important to connect optic fiber and patch cord from a smaller to a larger core size and from a lower NA to a higher NA to avoid light loss at the connection points. Optic fibers with a NA of 0.22 and 0.37 are commonly used. The NA determines the angles of light rays that are emitted from the optic fiber. Because of light scattering in brain tissue, the effect of the NA on the volume of illuminated brain tissue, is not important [19].

1.2.6 Methods of illumination

Different light sources can be used to obtain a precise spatiotemporal illumination of a target area within the brain tissue with specific wavelengths, for example: an arc lamp, LASER and LED [2, 19]. Each light source has advantages and disadvantages. It is possible to illuminate with a continuous bright light with an arc lamp, but its biggest disadvantage is its slow shutter control. On the other hand, a LASER has a better shutter control to control the timing of illumination. On top of this, a LASER illuminates with a high power collimated light and can be

efficiently coupled to optical fibers [29]. A LED can be also switched on and off rapidly, but in contrast with a LASER, it emits light in all directions rather than in a coherent beam, making effective transmission of light difficult [2].

1.2.7 Light stimulation parameters

Duration of illumination, both duration of a single pulse and pulse train, and stimulation frequency are important parameters in order to deliver efficient modulation [2, 12]. The impact of these parameters is not yet fully understood in optogenetics [2]. Hence it is necessary to determine these parameters to reach the optimal effect [12]. The number of AP is determined by the duration of a single pulse. Dependent on the ChR variant, a pulse of 1-2ms gives typically 1AP. Short light pulses (1-10ms at 20-70mW/mm^2) can be used to evoke activity from ChR2 expressing cells [20, 31]. Dependent on the properties of the targeted cell type, the stimulation frequency needs to be adjusted to reach the optimal effect. If it is possible, it is better to use lower frequencies to prevent any potential tissue damage [6, 12]. It is also important to limit pulse train duration, because a too long pulse train can lead to neurotransmitters run down and thus be inefficient [12].

The minimal required power (mW) of the light source to modulate neurons expressing opsins is another important parameter. It depends on the distance between the neurons expressing opsins and the optic fiber, due to limited penetrance of light into the brain. It also depends on light attenuation in brain tissue due to scattering [12, 26]. On top of this, there is loss of light due to light absorption by the brain tissue and as a result of the conical spreading of light after exiting the optic fiber [3, 26]. Moreover, the core size, NA and orientation of the optic fiber towards the transduced neurons has an effect on the minimal required power of the light source. If the optic fiber diameter is decreased, the threshold for modulation is also decreased. In addition, the minimal required power to modulate neurons expressing opsins is dependent on pulse duration, because an increasing pulse duration ensures a decreased threshold [26].

Furthermore, the chemistry of the opsin plays an important role in the choice of a stimulation protocol [2], because the light-sensitivity of the used opsin also plays an important role to determine the minimal required power. The following factors contribute to the light-sensitivity of an opsin: conductivity and kinetics of the opsin, density on the cell membrane which is related to the opsin expression level, number of ion channels illuminated and also the surface area [7, 26, 30, 32]. Opsins with a slower deactivation kinetics require lower intensities with longer light pulses for modulation [30]. The power must not exceed 100mW/mm^2 to avoid

tissue damage under long stimulation (>500ms) [6, 12, 20]. Thus, for safety, it is better to use powers up to 75mW/mm^2 for short light pulses (0.5 to 50ms) [6, 19, 20].

In common practice, AAV are injected into the brain, for example into the hippocampus or cerebral cortex, and subsequently the optic fiber is placed into the targeted brain area. Within this experiment, the illumination and stimulation of the targeted area, that will be in the cerebral cortex, will take place transvascularly through the superior sagittal sinus (SSS). Because of this, the optic fiber will be placed intravascularly into the SSS. The purpose of this will be explained in section 1.7. Hereby, it is also necessary to further clarify the blood supply of the brain and structure of the cerebral cortex, which will be discussed in section 1.3. Furthermore, stimulation of the targeted area with a specific wavelength causes evoked activity that can be measured with electrophysiological means such as electroencephalography (EEG) and unit recording, which will be also discussed in sections 1.5 and 1.6.

1.3 BLOOD SUPPLY OF THE BRAIN

1.3.1 Arterial system

The brain is supplied with blood through two vertebral arteries and two internal carotid arteries [8, 37]. The vertebral artery is a branch of the subclavian artery [37, 38]. The carotid arteries minister to the greatest part of blood supply of the supratentorial brain through the posterior cerebral artery and medial cerebral artery [8, 37]. The posterior cerebral artery originates from a connection branch from the internal carotid artery. Because of this, an anastomosis, the circle of Willis, is formed between the vertebral artery and the internal carotid artery which lies at the base of the brain [8, 37, 38]. The vertebral arteries come together just above the foramen

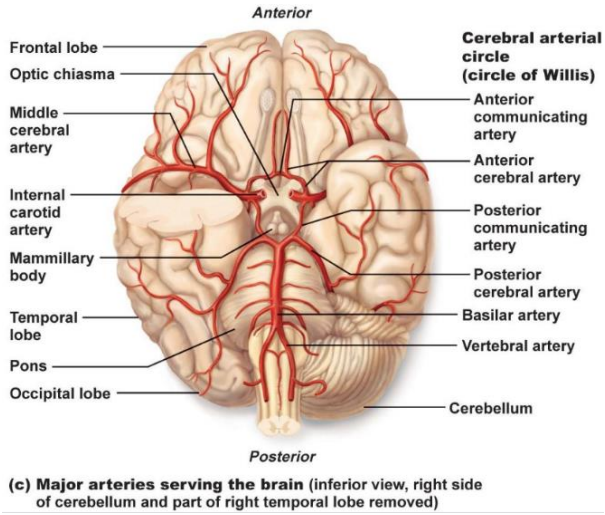

Figure 1: Blood supply of the brain: arterial system [37].

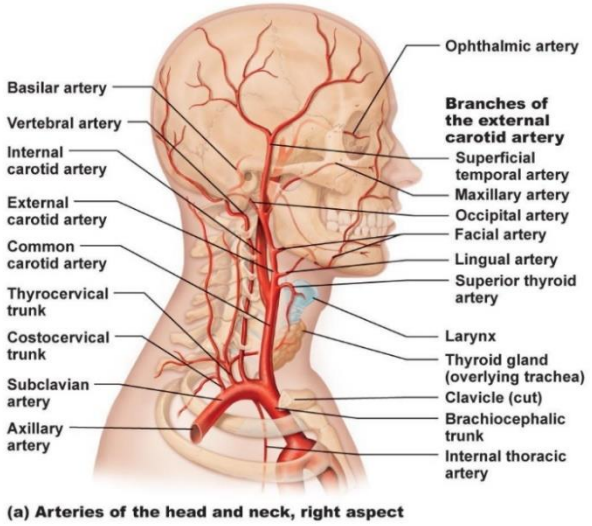

Figure 2: Blood supply of the brain: arterial system [37].

magnum and form the basilar artery, which supplies structures in the fossa posterior with blood. The basilar artery splits up in a left and right posterior cerebral artery, which supply the posterior part of the brain, above the tentorium, with blood (figure 1 and 2) [8, 37].

1.3.1 Venous system

The venous blood from the brain drains through a system of venous sinuses, which are situated around the brain, in the duplicated sheets of the dura mater. These venous sinuses drain in the internal jugular vein and vertebral vein [8, 37, 38]. One of the most important venous sinuses is the SSS, which is located in the falx cerebri between the two cerebral hemispheres, together with the inferior sagittal sinus. The inferior sagittal sinus drains posteriorly into the straight sinus. The SSS and the straight sinus drain posteriorly into the transverse sinuses. Each transverse sinus drains into the sigmoid sinus which becomes the internal jugular vein as it leaves the skull through the jugular foramen (figure 3) [37].

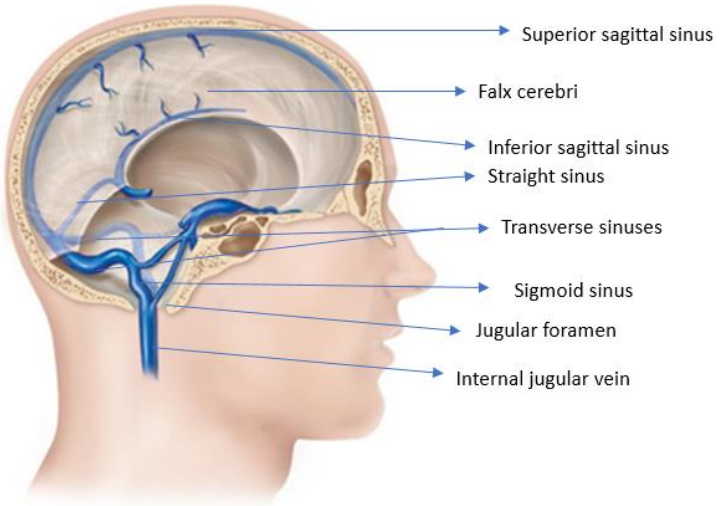

Figure 3: Blood supply of the brain: venous system [37].

1.4 CEREBRAL CORTEX

The neocortex is the largest part of the cerebral cortex and is made up of six distinct cell layers: the molecular layer (I), the external granular layer (II), the external pyramidal layer (III), the internal granular layer (IV), the internal pyramidal layer (V) and the multiform layer (VI), respectively from the outside to the inside [4, 39]. These different cell layers contain two general classes of neurons: principal neurons, often pyramidal neurons, which form excitatory synapses and interneurons, for example basket cells, which form inhibitory synapses [4, 20]. The balance between the excitatory and inhibitory system is important to avoid a hyperexcitable state which is related to epilepsy (see section 1.1 for more details in epilepsy) [4].

1.5 EEG

EEG is a tool to record pooled spontaneous electrical activity generated by a lot of simultaneously activated cerebral neurons with a high temporal resolution (ms). It measures field potentials, more specific post-synaptic potentials (PSP) and summated AP [1]. Also EEG can be seen as a graphic display of brain function recorded over time [11]. The rhythmic activity which can be seen on EEG is divided into different bands according to their frequency: delta (0-3Hz), theta (4-7Hz), alpha (8-13Hz) and beta (>14Hz) bands. Abnormal activity, for example spikes, sharp waves and spike-wave complexes, is present in epileptic patients on EEG [4]. The electrical activity of the brain can be measured from the scalp and within the brain, respectively scalp EEG and intracranial EEG.

1.5.1 Scalp EEG

EEG is recorded from the surface of the scalp and not in the deepest sulci, with scalp electrodes. Electrodes are placed on standardized positions on the scalp. In humans, this placement is according to the International 10-20 System. In experiments with laboratory animals, these scalp electrodes are positioned at locations of interest. EEG represents the electrical function of the brain, but not its anatomy [8, 11].

1.5.2 Intracranial EEG

Intracranial EEG can be recorded with different kinds of electrodes, for example: intraparenchymal depth electrodes, linear subdural strip electrodes and grid electrodes. If the electrical activity is recorded from deeper locations within the brain, closer to the cerebral neurons, via the insertion of a depth electrode, local field potentials (LFP) are measured. Microelectrodes are used to record single cell activity at locations of interest (section 1.6) [11].

If electrical activity is recorded directly from the surface of the cerebral cortex with a higher spatial resolution, it is called electrocorticography. This can be accomplished by using both strip and grid electrodes [11].

1.6 UNIT RECORDING

Responses of one or a few neurons can be recorded with unit recording, respectively single-unit and multi-unit recording. For single unit recordings, the recorded signal of a few neurons is band pass filtered between 300Hz (low pass filter) and 5kHz (high pass filter) to obtain a signal of one neuron. The physiology, connectivity and cell activity of individual neurons can be studied with single-unit recording. Also the effect of cell activity on behaviour or physiology

can be determined through stimulation of that individual neuron. To study the functioning of neuronal circuits, multi-unit recording is more appropriate [40].

It is possible to record responses of neurons extracellularly or intracellularly with unit recording. Synaptic potentials below the threshold that influence cell excitability without provoking AP need to be recorded intracellularly. Intracellular unit recording can be more easily conducted in *in vitro* set-ups. Extracellular unit recording can only measure evoked activity under the form of AP or spikes. During these measurements, PSP are filtered away [40].

AP or spikes are provoked by a depolarization of the neuronal membrane above the threshold. The membrane potential is affected by the activation of ligand-gated channels, voltage-gated channels and changes in intracellular ion compartmentalization. As a result of AP, neurotransmitters are released. The most important neurotransmitters in the brain are: glutamate, GABA, acetylcholine, norepinephrine, dopamine, serotonin, and histamine. Glutamate is an excitatory neurotransmitter that binds on the following ionotropic glutamate receptors: alpha-amino-2,3-dihydro-5-methyl-3-oxo-4-isoxazolepropanoic acid (AMPA) receptors, kainic acid (KA) receptors, and N-methyl-D-aspartate (NMDA) receptors, which are permeable to Na^+ and K^+ ions. Glutamate can also bind on metabotropic receptors. From several experimental studies, it is known that NMDA, AMPA and KA agonists can induce seizure activity and are thus used as animal models of epilepsy. GABA is an inhibitory neurotransmitter that binds on $GABA_A$ receptors, which are permeable to Cl^- ions, and $GABA_B$ receptors. $GABA_A$ receptor agonists are known to supress seizure activity. An imbalance between the glutamatergic system and the GABAergic system plays an important role in epilepsy (section 1.1) [4].

1.7 PURPOSE AND DEFINITION OF THE PROBLEM

Epilepsy is a chronic neurological disorder characterized by repeated and spontaneous epileptic seizures due to a hypersynchronous neuronal activity in a hyperexcitable neuronal network in the brain [1, 4]. Current treatments such as AEDs, resective or disconnection surgery and neurostimulation do not always have the desired effect or patients are experiencing too many adverse side-effects [1-3, 15]. Hence it is necessary to develop new anti-epileptic therapies. One of them is optogenetics, which provides a spatiotemporal and cell-type specific control of neuronal activity with light and opsins [2, 18]. Because of the more precise mechanism of action, optogenetics may be more effective and minimize the adverse side-effects [15]. But, a current hurdle is the invasive nature of optogenetics as an optic fiber needs to be implanted into the brain.

Transvascular optogenetic stimulation could allow a less invasive approach to light delivery. In contrast with common practice, the optic fiber is placed intravascularly. With this technique, trauma of brain tissue during insertion of the optic fiber, that may result in inflammation, gliosis and disruption of the blood-brain barrier could be avoided. The most severe side-effect of placing the optic fiber in this cerebral vein is venous thrombosis, although the chance that this will happen is quite small [41].

Previous research shows that duration of illumination, stimulation frequency and LASER output power are important parameters for optogenetic stimulation. But the impact of these parameters is not yet fully understood in optogenetics. So it is necessary to determine these parameters to reach an optimal effect [2, 12, 26].

It was hypothesized that short pulses can be used to modulate ChR2 and GtACR2 expressing neurons (1-10ms and 10ms respectively) [20, 28, 31]. The optimal stimulation frequency depends on the cell type that is illuminated, but is it better to use lower frequencies if possible to avoid tissue damage [6, 12]. The minimal required power to modulate ChR2 and GtACR2 expressing neurons depends on the distance between the optic fiber and the stimulated ChR2 or GtACR2 expressing tissue [12, 26]. The minimal required power also depends on the pulse duration: an increasing pulse duration ensures a decreased modulation threshold [26]. The modulation threshold depends on the conductivity and kinetics of the opsin, density of opsin expressing tissue, number of ion channels illuminated and the surface area [7, 26, 32].

The goal of this study is to determine if transvascular optogenetic stimulation is possible. Therefore, ChR2 expressing cortical tissue will be stimulated with blue light (470nm) with an intravascular optic fiber, placed against the ipsilateral wall of the SSS. If transvascular optogenetic stimulation is possible, the minimal required power, optimal pulse duration and optimal stimulation frequency to modulate ChR2 and GtACR2 expressing neurons next to the SSS will be determined. Furthermore, it will be investigated if the evoked activity can be detected using electrophysiological means such as EEG and unit recording. Moreover, the maximal distance at which modulation of neurons expressing the opsins is still possible will be determined. The capacities of GtACR2 to inhibit neural activity will be explored too. The expression of the opsins will be validated through an immunofluorescence staining. The spatial extent of ChR2 and GtACR2 expressing cortical tissue will also be determined. On top of this, double stainings for GFP/NeuN and mCherry/NeuN will be conducted to test for colocalization and toxicity. The staining for VGluT1 will also be optimized, because this could allow for a better visualisation of colocalization.

2 MATERIALS AND METHODS

2.1 LABORATORY ANIMALS

Nine male Sprague-Dawley rats (Envigo, The Netherlands) weighing between 230-350g were used. During the experiments, the animals were housed in group in the central animalarium of UZ Ghent in type III cages (Makrolon Technilab). Food and water were provided ad libitum. The cages were also enriched with nesting material. The animals were kept in a controlled environment: 20-22°C, a relative humidity of 40-55% and a 12h light/12h dark cycle. All the experiments took place during the light phase of the light/dark cycle. The animals were treated according to the European guidelines and standards. The experiments were approved by the animal ethical comite (ECD 16/31) of Ghent University.

2.2 LASER

Before the experiments were started, the output powers (mW) of a LASER (BL473T3-050FC, Shanghai Laser Systems, blue light, 470nm) attached to a 50µm patch cable (NA= 0.22) and optic fiber (diffuse light, core diameter= 60µm, outer diameter= 75µm, NA= 0.22, doric lenses, MFC_060/075-0.37_20mm_ZF1.25_DFL) during continuous illumination and during illumination with different pulse durations (1ms, 3ms, 10ms and 25ms pulses) were determined. The output power was measured using a watt-meter (PM100A, Thorlabs). It is important to keep the optic fiber clean to ensure maximal light output power, and to test the light output power before the start of each experiment [20].

2.3 SURGERY ONE: AAV INJECTION

2.3.1 In General

AAVs were injected into the neocortex of male Sprague-Dawley rats next to the SSS. As a result, the excitatory pyramidal neurons of the neocortex specifically expressed the opsins. In rat 1-3, a rAAV5/CamKIIα-hChR2(H134R)-eYFP (titer not known) vector was injected and in rat 4-9, an AAV2/5 CaMKII0.4-intron-hGtACR2-mCherry vector (titer= $1{,}82*10^{12}$ genome copies/ml (gc/ml)) was injected.

2.3.2 Protocol

Before surgery, all the required material was gathered and disinfected with 70% ethanol. Also the chirurgical site was prepared and disinfected. The AAV was get out of the -80°C freezer, loaded into the nanoject II device (Drummond Scientific, Broomall, PA,USA) and put on ice. Before surgery, the rats were induced with 5% isoflurane (IsoFlo®, Zoetis, Belgium) mixed with medical oxygen (8l/min). Next the rats were weighed and fixed in the stereotactic frame (Bilaney Consultants, Düsseldorf, Germany) on a heating pad and were given a subcutaneous (SC) injection on top of the skull of xylocaine mixed with adrenalin (1mg/kg, AstraZeneca, Belgium) for extra local anaesthesia and vasoconstriction (figure 4). Duratears (Alcon®) was applied on the eyes to prevent dehydration. During surgery, anaesthesia was maintained with 2% isoflurane (IsoFlo®, Zoetis, Belgium) mixed with medical oxygen (1l/min) and the rectal temperature of the rats was measured (DC Temperature Controller). After shaving and disinfecting the scalps of the rats, a longitudinal incision was made on the scalp with a scalpel and the periost was removed. Next, the coordinates of bregma (intersection of coronal and sagittal suture) and lambda (intersection of sagittal and occipital suture) were measured with a marker using the stereotactic frame (figure 5) [42]. When bregma and lambda were brought on the same height, the surgery was preceded. Next, the vector injection site towards bregma (AP: -4.2mm, ML: 0.5mm) was stereotactically determined with a marker. Here, a craniotomy was made up to the dura mater. Then, the coordinates of bregma were determined with the nanoject and the nanoject was moved towards the injection site. The AAV vector was injected 1mm (10*50.6nl, every 10'') and 0.5mm (10*50.6nl, every 10'') under the dura mater (DV: 0.5mm and 1mm) with the nanoject. After keeping the nanoject in place for 5', it was pulled out of the injection site (figure 6) [15, 43]. Next, kwik-syl was applied on the craniotomy, and the rats were stitched (Silkam 5/0 wire). After this surgery, metacam (1mg/kg, nonsteroidal anti-inflammatory drug, Boehringer Ingelheim, Germany) was injected SC.

Figure 4: Setup for surgery: stereotactic frame and heating pad.

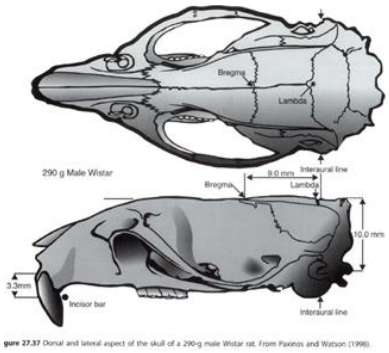

Figure 5: Position of bregma and lambda on the rat skull [42].

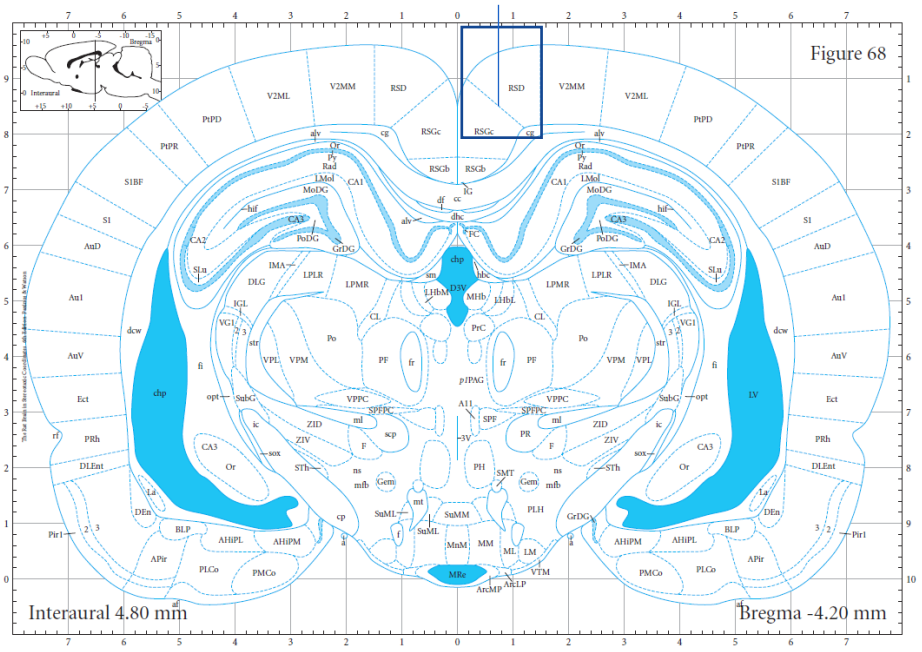

Figure 6: Injection site in the rat. Coordinates: AP: -4.2mm, ML: 0.5mm, DV: 1mm and 0.5mm [43].

2.4 SURGERY 2: RECORDINGS

2.4.1 In general

During a second surgery, two weeks after transduction [5, 16], the optic fiber was placed intravascularly, against the ipsilateral wall of the SSS. As a result, the activity of the genetically modified neurons could be manipulated transvascularly with blue light (470nm) through this optic fiber.

2.4.2 Protocol

Before surgery, all the required material was gathered and disinfected with 70% ethanol. Also the chirurgical site is prepared and disinfected. The impedance of the Tungsten micro-electrode (75µm) soldered to two connector pins was measured with the electrode impedance tester (bak electronics, inc). When the impedance is above 1MΩ, the electrode can be used during surgery. The first steps of this surgery, from induction of anaesthesia to removal of the periost, were the same as described in 2.3.2, except that

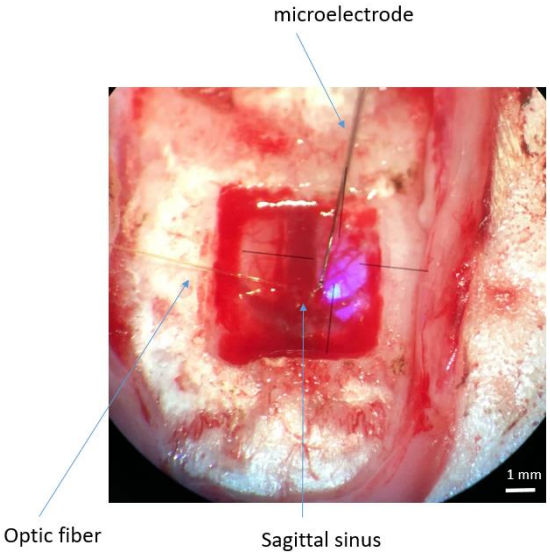

Figure 7: Placement of the microelectrode in the rat brain and the optic fiber in the superior sagittal sinus.

anaesthesia was maintained with 1.5-2% isoflurane mixed with medical oxygen (1l/min) in this surgery. Next, it was validated whether bregma and lambda were on the same height and a bigger craniotomy was made around the injection site and two holes were drilled in the frontal skull bone. Two screws were placed into these holes, connected to conductive wire and served as reference and ground. The Tungsten microelectrode was put into or close to the injection site to measure evoked activity in response to blue light illumination (figure 7). The micro-electrode and the screws were connected to a pre-amplifier and amplifier. For single unit recordings, the recorded signal was band pass filtered between 300Hz (low pass filter) and 5kHz (high pass filter). The amplification was set on x10000. For LFP, the low pass filter was set on 1Hz and the high pass filter on 5kHz. The amplification was set on x500. Next, the optic fiber connected to a fiber-optic path cord and coupled to the LASER was placed into the SSS from the lateral side against the ipsilateral wall of this cerebral vein (figure 7). The opsins were stimulated with Neuron, software in MATLAB, with different output powers to study the effect of stimulus intensity, pulse durations and stimulation frequencies. During this stimulation, micro-electrode was placed at specific depths and distances from the SSS (figures 8 and 9).

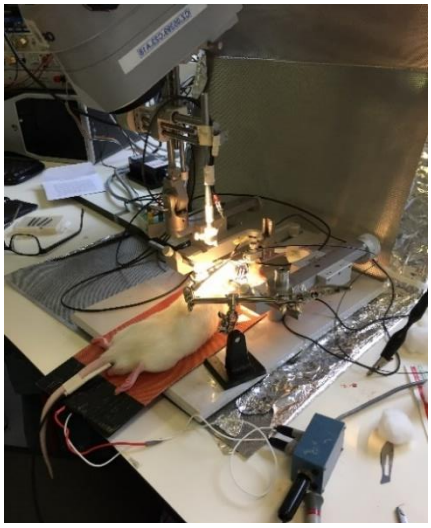

Figure 8: Setup for surgery.

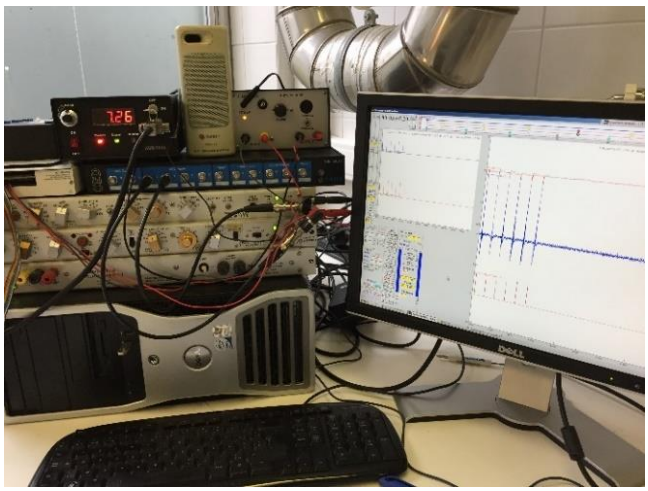

Figure 9: Measurements in Neuron in MATLAB.

The following stimulation protocol was used in rat 1-6 at different depths and distances from the SSS (table 1):

- EP burst: 6 pulses of 1ms at 50Hz, 100Hz, 200Hz and sometimes 400Hz, LASER output 18.2mW
- IO burst: 6 pulses of 1ms at 100Hz, LASER output 0.1mW to 18.2mW
- IO: 1 pulse of 1ms, 3ms, 10ms and 25ms, LASER output 0.1mW to 18.2mW, 0.3mW to 24.0mW, 0.3mW to 31.7mW and 0.5mW to 33.4mW respectively.

On top of this, in rat 4, one long pulse of 1000ms was given. In rat 6 the following stimulation parameters were also tested: 1000ms pulses at 0.1Hz and 100ms pulses at 5Hz. Both of them were tested from LASER output 0.3-19mW. Furthermore, 10ms pulses at 50Hz LASER output 2.2mW and 32.2mW were also tested.

After testing this stimulation protocol, 50nl of KA (200ng) was applied to the cortex in rat 5 and 6 to increase the activity of the cortical neurons. Then, the following stimulation parameters were tested in rat 5: 1000ms pulses at different intensities (LASER output 0.3-19mW), 2000ms pulses, 4000ms pulses, 100ms pulses, 500ms pulses, 750ms pulses, 10ms pulses (all at 19mW) and continuous illumination at low and high intensities (LASER output 2mW, 15mW and 19mW). In rat 6, 100ms pulses at 5Hz LASER output 19mW and 2000ms pulses at 0.1Hz LASER output 19mW were tested.

The following stimulation protocol was used in rat 7-9 before and after application of KA (table 1):

- IO burst: 6 pulses of 1ms at 5Hz, 20Hz, 50Hz, 100Hz and 200Hz, LASER output 0.1mW to 18.2mW
- IO: 1 pulse of 1ms, 3ms, 10ms, 25ms, 1000ms and 2000ms, LASER output 0.1mW to 18.2mW, 0.3mW to 24.0mW, 0.3mW to 31.7mW and 0.5mW to 33.4mW respectively. LASER outputs for 1000ms and 2000ms pulses were equated to LASER outputs for continuous illumination: 0.3mW to 19mW
- Stim: 3’ stimulation (4” OFF – 56” ON – 4” OFF – 56” ON – 60” OFF) at 5Hz, 20Hz, 50Hz and 100Hz, LASER output 2.3mW and 19mW, 2.2mW and 33.4mW, 2.2mW and 31.7mW, ~2mW and ~30mW respectively.

Rat 7 received 50nl KA, rat 8 two times 50nl KA and rat 9 three times 50nl KA.

Table 1: Summary table about the repeatedly used stimulation paradigms.

Stimulation paradigm	Number of pulses	Pulse duration (ms)	Frequency (Hz)	LASER output power (mW)
EP burst	6	1	50, 100, 200, 400	18.2
IO burst	6	1	5, 20, 50, 100, 200	0.1-18.2
IO	1 1 1 1 1 1	1 3 10 25 1000 2000	/ / / / / /	0.1-18.2 0.3-24.0 0.3-31.7 0.5-33.4 0.3-20 0.3-20
Stim	3’ stimulation: 4”OFF-56”ON- 4”OFF-56”ON- 60”OFF	100 25 10 5	5 20 50 100	2.3 and 19 2.2 and 33.4 2.2 and 31.7 ~2 and ~30

2.4.3 Outcome

Evoked potentials (EP) were induced by each pulse of blue light with sufficient intensity (470nm) and were evident on LFP and extracellular single unit recording. Recording and stimulation was controlled by custom software (Neuron) designed in MATLAB.

2.4.4 Data analysis

The collected data were analysed with custom software (Neuron) designed in MATLAB. For both ChR2 and GtACR2, the amplitudes (mV) of the LFP (black) were measured from the beginning of the stimulation to the deepest point. A line was drawn with Neuron at the start of the stimulation to make this more clear. On top of this, the EP duration (ms) was also measured with Neuron (figure 10 and 11). With these data, graphs were made in excel. For GtACR2 alone, AP (peaks) were counted in the raw signal (figure 12). The inhibition during stimulation after application of KA was measured qualitatively.

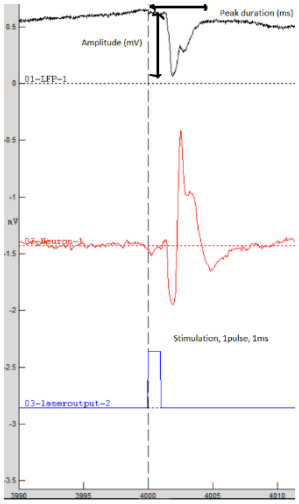

Figure 10: Example of an IO measurement with one 1ms pulse, LASER output 7.3mW. The amplitude (mV) and duration (ms) (black arrows) of the local field potential (black) in response to blue light stimulation (blue) were measured. As help, a line was drawn at the beginning of stimulation (4000ms).

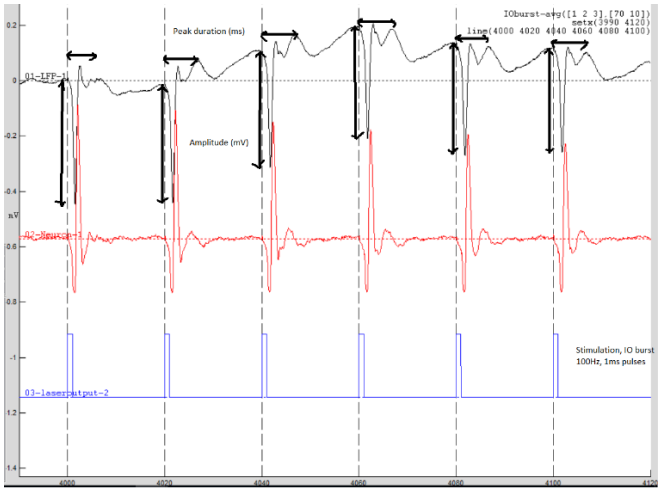

Figure 11: Example of an IO burst measurement at 100Hz, LASER output 10.2mW. The amplitudes (mV) and durations (ms) (black arrows) of the local field potentials (black) in response to blue light stimulation (blue) were measured. As help, lines were drawn at each beginning of stimulation (4000ms, 4020ms, 4040ms, 4060ms, 4080ms and 4100ms).

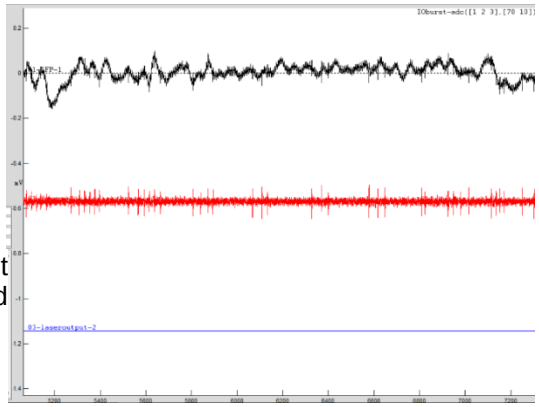

Figure 12: Example of an IO burst measurement at 20Hz, LASER output 10.2mW. AP were counted in the raw signal (peaks).

2.4.5 Transcardial perfusion

The rats were transcardially perfused after the second surgery. Before surgery, phosphate buffered saline (PBS) and 4% phosphate buffered paraformaldehyde (PB-PFA) were made. For PBS, a stock solution of PB (0.2M, pH 7.4) was made: 42.6g of Na_2HPO_4 was diluted in 1.5l distilled water (dH_2O) (dibasic solution) and 12g of NaH_2PO_4 was diluted in 0.5l dH_2O (monobasic solution). The monobasic solution was slowly added to the dibasic solution until a pH of 7.4 was reached. Next, this stock solution of PB was diluted twenty times in dH2O (50ml PB in 950ml dH_2O) and 9g NaCl was added. For 4% PB-PFA: at day one, 350ml dH_2O was added to 500ml stock solution PB and pre-heated till 50°C (maximum 60°C). Then, 40g PFA was added and mixed until it was completely dissolved. This solution was stirred with a magnetic bar for a whole day without being heated. At day two, the solution was filtered and 150ml dH_2O was added. The solution needs to be clear and can be kept on 4°C. Just before the perfusion, two infusion bags, one with PBS (300ml) and one with 4% PB-PFA (300ml), were filled. Next, ketalar (100mg/kg, Pfizer) and an overdose of anaesthetic, dolethal (1ml/1.5kg, Vétoquinol), was injected intraperitoneally. If the breathing is stopped, heparine (0.2ml) was injected in the apex of the beating heart to prevent coagulation and a small incision in the right atrium was made. The transcardial perfusion started with PBS (10') and then continued with 4% PB-PFA (10'). Therefore, a needle attached to the infusion bags of PBS and PB-PFA was put into the aorta via the apex of the heart and the solutions were spread into the body of the rats. PBS was used to remove all the blood out of the body and PB-PFA for fixation.

2.5 HISTOLOGY

2.5.1 Isolation, snapfreeze and cryosections

The rat brains were isolated after perfusion and post-fixated 24-48h in 4% PB-PFA at 4°C. The fixated brains were successively embedded in a 10%, 20% and 30% PBS-sucrose solution for cryoprotection. The brains were kept in these solutions until they were saturated. Next, they were snapfreezed in isopentane cooled in liquid nitrogen and preserved at -80°C. Antifreeze medium was prepared before cryosectioning: 1.7g $NaH_2PO_4.H_20$ and 5.45g $NA_2HPO_4.2H_2O$

Figure 10: Cryosectioning using the Leica CM 3050 S Cryostat.

were dissolved in 400ml dH_2O. Next, 300ml ethylene glycol and 300ml glycerol were added to the solution and stirred. The rat brains need to be moved from -80°C to -20°C at least 1h before cryosectioning. Sequential cryosections of 40µm were made using the Leica CM 3050 S Cryostat and stored in antifreeze medium at 4°C (figure 13). About 144 cryosections where made from each animal around the injection site.

2.5.2 Immunofluorescence staining

Seven sections per animal (every five sections from 600µm before to 600µm after the injection site, one section was selected) were selected for immunofluorescence staining and tested for opsin expression. The rest of the slices were stored in antifreeze medium at -20°C. The brain slices were washed in dH_2O (2 x 5'), then in 0.5% H_2O_2 (30') and in 1% H_2O_2 (60'). H_2O_2 is used to block endogenous peroxidase activity. Next, brain slices were washed in PBS (2 x 5') and blocked in blocking buffer (45', BB, PBS with 0.4% Fish Skin Gelatin and 0.2% Triton X). BB occupies all the binding sites and competes with the primary antibodies. Subsequently, the brain slices were incubated in primary antibodies in BB for 1h at room temperature and were then placed in the fridge (4°C) overnight. The following primary antibodies were used: chicken polyclonal anti-GFP (1/1000, against eYFP, AB16901, Sigma-Aldrich) and rabbit polyclonal anti-red fluorescent protein (RFP) (1/1000, against mCherry, AV34144, Sigma-Aldrich). Mouse monoclonal anti-NeuN (neuronal marker, 1/500, MAB377C3, Sigma-Aldrich) was used as positive control. BB alone was used as negative control. After this incubation, the brain slices were washed in BB (2 x 10'). During the next steps, the slices were placed in the dark to prevent photobleaching (fluorescence loss). Next, the brain slices were incubated in the secondary antibodies in BB for 1h at room temperature. The following secondary antibodies were used: Alexa fluor goat anti-chicken (1/1000, 594 nm, Sigma-Aldrich), Alexa fluor goat anti-rabbit (1/1000, 594nm, Sigma-Aldrich), Alexa fluor goat anti-mouse (1/1000, 488nm, Sigma-Aldrich). Further, the brain slices were washed in PBS (2 x 5') and a nuclear staining with DAPI in PBS was performed (1' at room temperature, 5mg/ml stock solution, 5ml solution of 1µg/ml). The brain slices were washed again in PBS (2 x 5') and mounted on glass microscope slides with Vectashield Mounting Medium Fluorescence, coverslips and nail polish. The brain slices were stored at 4°C.

On top of this, a double staining was performed for NeuN/GFP and NeuN/mCherry to test for colocalisation and toxicity on three sections per animal. For this, the following combinations of primary and secondary antibodies were used:

- NeuN/GFP: mouse monoclonal anti-NeuN (1/500, MAB377C3, Sigma-Aldrich) + rabbit polyclonal anti-GFP (1/1000, AB3080, Sigma-Aldrich) and Alexa fluor goat anti-mouse (1/1000, 594nm, Sigma-Aldrich) + Alexa fluor goat anti-rabbit (1/1000, 488nm, Sigma-Aldrich)
- NeuN/mCherry: mouse monoclonal anti-NeuN (1/500, MAB377C3, Sigma-Aldrich) + rabbit polyclonal anti-RFP (1/1000, AV34144, Sigma-Aldrich) and Alexa fluor goat anti-mouse (1/1000, 488nm, Sigma-Aldrich) + Alexa fluor goat anti-rabbit (1/1000, 594nm, Sigma-Aldrich)

Mouse monoclonal anti-NeuN (1/500, MAB377C3, Sigma-Aldrich) and Alexa fluor goat anti-mouse (1/1000, 488nm, Sigma-Aldrich) were used as positive control. The secondary antibodies alone were used as negative control.

Furthermore, the immunofluorescence staining with VGluT1 was optimized. The VGluT1 antibody is directed against exciting glutamatergic neurons. Goat anti-VGluT1 (Sigma-Aldrich) was used as primary antibody. Different dilutions were tested: 1/1000, 1/2000, 1/5000, 1/7500, 1/10000 and 1/15000. Alexa Fluor rabbit anti-goat (1/1000, 488nm, Sigma-Aldrich) was used as secondary antibody.

2.5.3 Fluorescence microscopy

Opsin expression was visualized with a fluorescence microscope (Carl Zeiss, Axiovert 200M and Nikon Eclipse TE2000-E). Pictures of DAPI, NeuN, GFP and mCherry were taken with the AxioVision Microscope Software (6D acquisition) connected to the Carl Zeiss fluorescence microscope on the 4x, 10x, 20x and 40x magnification and with the Nis-Elements F software connected to the Nikon fluorescence microscope on the 20x magnification. Because GFP was stained in red during the first immunofluorescence staining, the colour was changed from red to green with the AxioVision Microscope Software. Pictures were saved as ZVI-file and exported to a TIF-file.

2.5.4 Histological analysis

Measurements of the spatial extent of opsin expression were performed in ImageJ. The scale was set on following specifications for each opsin:

- GtACR2:
  - Scale bar = 200µm ~ 75 = distance in pixels
  - Known distance = 0.2
  - Unit = mm
  - Pixel aspect ratio = 1.0

- ChR2:
    - Scale bar = 100µm ~37.5 = distance in pixels
    - Known distance = 0.1
    - Unit = mm
    - Pixel aspect ratio = 1.0

A line was drawn around the expression area, which was measured with the area function in ImageJ. Then, the expression volume was calculated per segment (blue) based on the expression area of each slice (seven per animal) and the known distance between the slices (160µm) (figure 14).

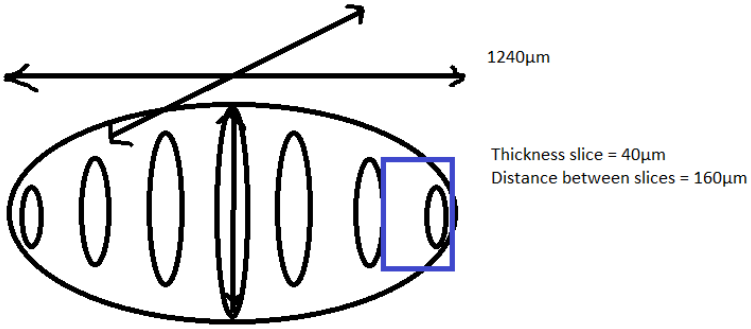

Figure 11: Scheme histological analysis. The expression volume was calculated per segment (blue) based on the expression area of each slice and distance between the slices (160µm).

Pictures of the GFP/NeuN double staining (20x magnification with Carl Zeiss, Axiovert 200M microscope) were analyzed with Fiji, an upgraded version of ImageJ to check for colocalization. Cell bodies on the GFP pictures were counted, markers were set on it and copied to the NeuN pictures. Because of these markers, the number of double positive cells could be counted and also the ratio of double positive cells could be calculated (figure 15). Pictures of the mCherry/NeuN double staining (20x magnification, Nikon Eclipse TE2000-E microscope) were merged with Fiji to check for colocalization.

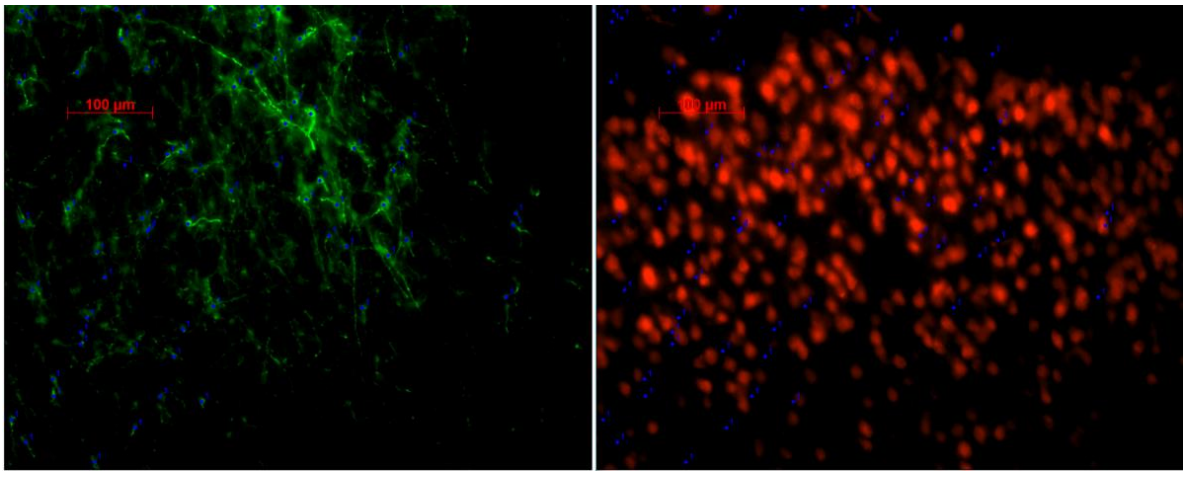

Figure 12: Histological analysis of GFP/NeuN double staining in Fiji. Cell bodies on the GFP picture (left) were counted (blue dots) and copied to the NeuN picture (right) (blue dots) to check for colocalization.

3 RESULTS

3.1 LASER

The output powers (mW) and the analog outputs (mV) of the LASER attached to a 50µm patch cable and optic fiber during continuous illumination and illumination with different pulse durations (1ms, 3ms, 10ms and 25ms pulses) were determined (table 2).

Table 2: Power measurement (mW) and analog output (mV) during illumination with different pulse durations (1ms, 3ms, 10ms and 25ms) and continuous illumination with the LASER coupled to the optic fiber. The output power during continuous illumination was measured before each experiment and the average was calculated of these measurements. The analog output during continuous illumination was calculated using the following equation: $y= 0.074x – 0.0465$ ($R^2=1$).

Illumination	1ms		3ms		10ms		25ms		continuous	
LASER knob	mV	mW	mV	mW	mV	mW	mV	mW	mV	mW
10	250	18.175	330	23.991	436	31.6972	460	33.442	257.4	19
9	170	12.359	240	17.448	310	22.537	370	26.899	223.6	16.5
8	140	10.178	185	13.4495	230	16.721	260	18.902	2033	15
7	101	7.3427	115	8.3605	130	9.451	160	11.632	135.8	10
6	50	3.635	65	4.7255	75	5.4525	80	5.816	81.7	6
5	15	1.0905	25	1.8175	30	2.181	30	2.181	31.0	2.25
4	2,5	0.18175	3.5	0.25445	4	0.2908	7	0.5089	5.2	0.34

3.2 TRANSVASCULAR OPTOGENETIC STIMULATION

First of all, it was determined if transvascular optogenetic stimulation is possible. For this, the optic fiber was placed intravascularly, against the ipsilateral wall of the SSS. The neocortex expressing ChR2, was then stimulated with blue light (470nm) transmitted by this intravascular optic fiber with different stimulation protocols (see section 2.4.2). EP were provoked in the ChR2 expressing tissue in response to blue light transmitted by the intravascular optic fiber, which means that transvascular optogenetic stimulation is possible.

3.3 OPTIMAL STIMULATION PARAMETERS

In this experiment, stimulation of ChR2 expressing tissue did not provoke AP and no single unit activity could be recorded. In contrast to ChR2 experiments, we were able to record AP in GtACR2 stimulation experiments. Provoking AP does not depend on the depth, stimulation frequency or LASER output power. In this way, AP could be provoked during all different

measurements (see section 2.4.2). Neurons could also be turned on during all these stimulation protocols, accompanied by a large increase of AP. The evoked activity could be detected as LFP, both with ChR2 and GtACR2.

3.3.1 Output power and pulse duration

It was hypothesized that the minimal required power to modulate ChR2 and GtACR2 expressing neurons depends on the distance between the optic fiber and the stimulated ChR2 or GtACR2 expressing tissue. On top of this, it was also hypothesized that EP amplitudes rise with an increasing output power (figure 16). To determine this, EP amplitudes (mV) at different depths were plotted against LASER output powers (mW). Graphs were made per pulse duration (1ms, 3ms, 10ms, 25ms, 1000ms and 2000ms) and output powers for the specific pulse durations were put on the x-axis. For the 1000ms and 2000ms graphs, the output powers for continuous illumination were used (table 2 in section 3.1). With these graphs, it was also possible to determine if the EP amplitudes depend on the depth (figures addendum).

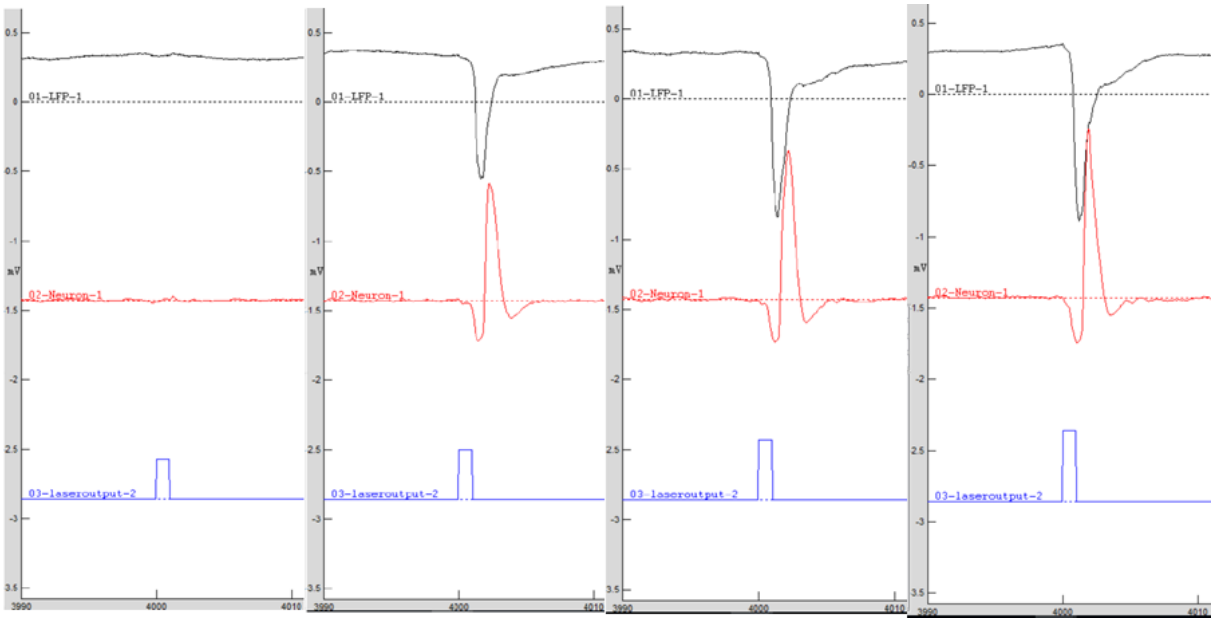

Figure 13: Example of an IO measurement for GtACR2 at 0.6mm under the dura mater. One pulse of 1ms (blue) was given at 0.2mW - 1.1mW - 3.6mW - 7.3mW from left to right respectively. Local field potentials were provoked (black) in response to the light stimulus from 1.1mW.

It appeared from the measurements taken with the micro-electrode placed at specific depths and distances from the SSS that modulation of ChR2 expressing neurons is possible up to a depth of 1.5 to 2.5mm under the dura mater and 0.9 to 1.3mm lateral to the edge of the SSS. For the depth, eleven measurements in discrete steps were conducted from 0.7-2.5mm under the dura mater and for the distance, 4 measurements were carried out from 0.1-1.3mm lateral to the edge of the SSS. Furthermore, it appeared that GtACR2 can be activated up to a depth

of 1.9 to 2.1mm under the dura mater and 0.6 to 0.9mm lateral from the edge of the SSS (figures addendum). Herefore, 12 measurements from 0.4-2.1mm under the dura mater and 3 measurements 0.4-0.9mm lateral from the edge of the SSS were conducted in discrete steps.

The results of this study show that EP amplitudes, if EP are provoked, do not depend on the depth (figures addendum). Because of this, it was decided to normalize EP amplitude data and plot these data for all neurons for each pulse duration against the output powers for continuous illumination. Because it was hypothesized that a longer pulse duration and a greater LASER output power provoke EP with the biggest amplitude, the EP amplitudes were normalized to the 25ms pulse stimulation at 19mW (=1) (figures 17 and 18).

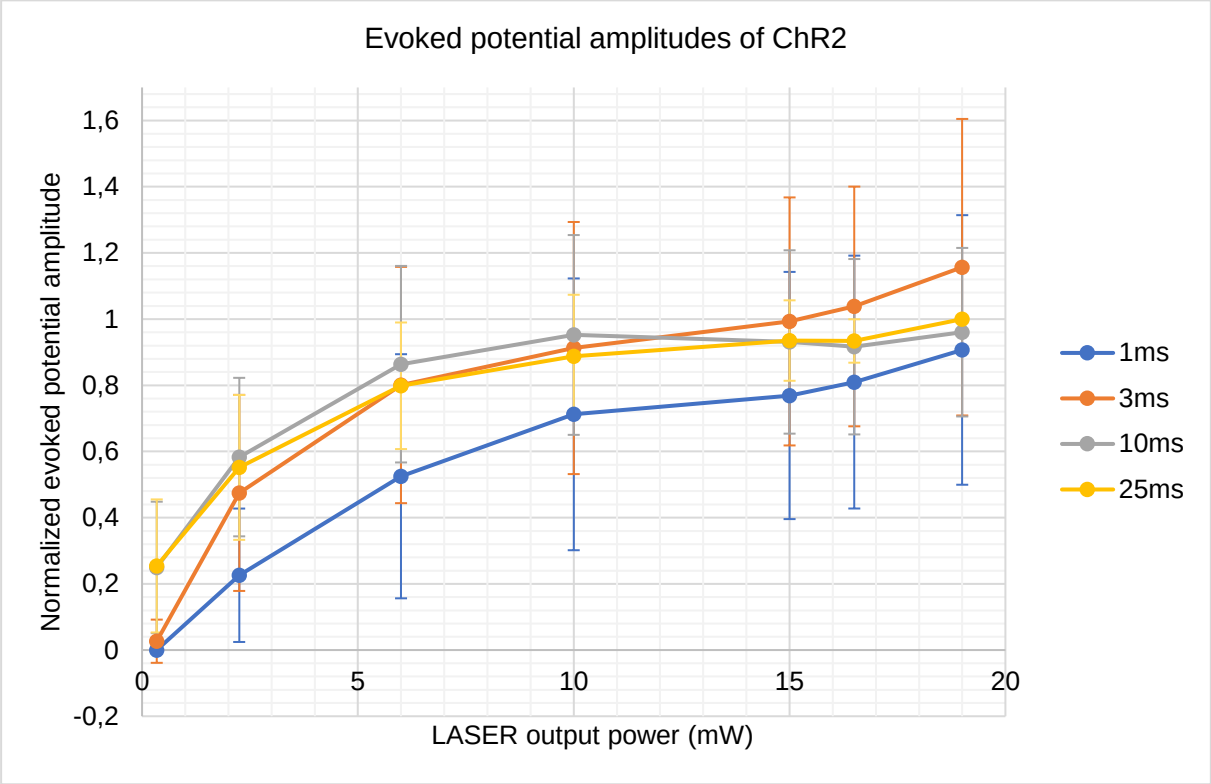

Figure 14: Evoked potential (EP) amplitudes of ChR2 expressing neurons at different pulse durations (1ms, 3ms, 10ms and 25ms). The LASER output powers (mW) for continuous illumination were set on the x-axis. The EP amplitudes were normalized to the 25ms pulse stimulation at 19mW (=1) (y-axis). The average EP amplitudes were plotted against the LASER output powers. Error bars (standard deviations) were put on the graph as well.

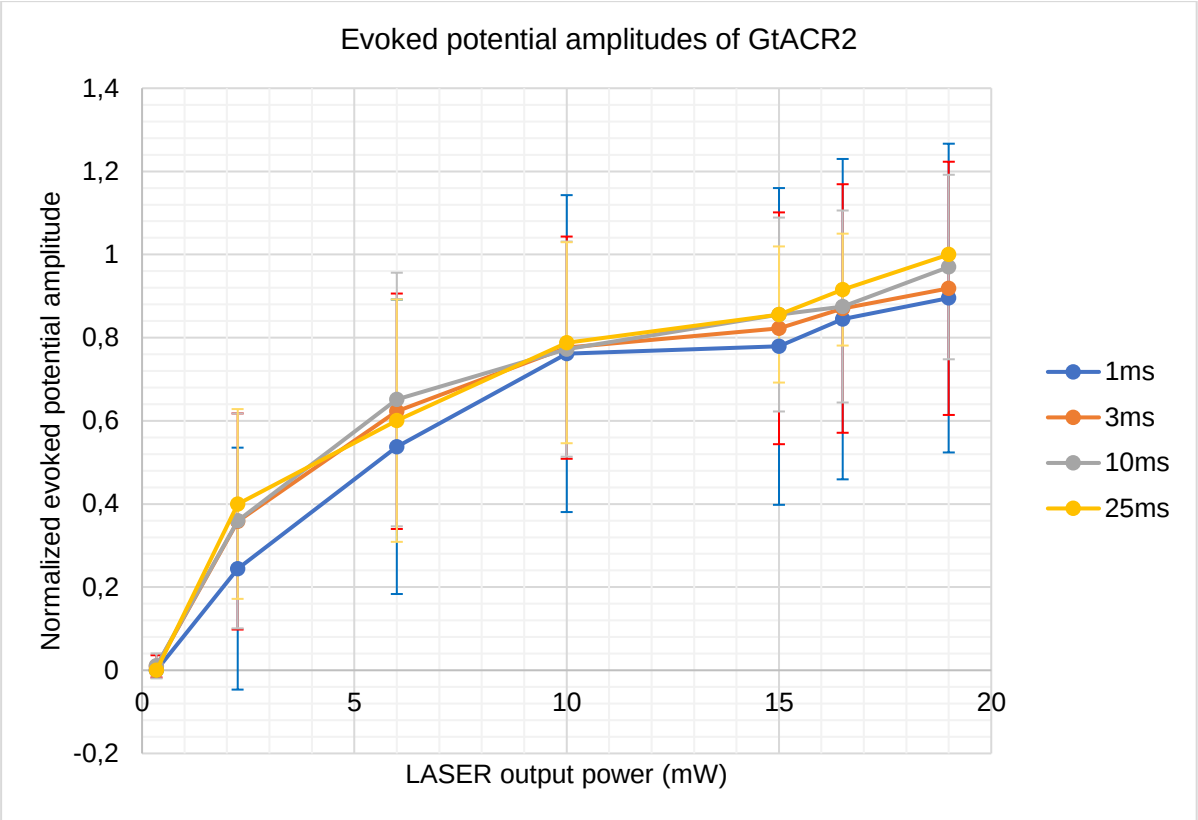

Figure 15: Evoked potential (EP) amplitudes of GtACR2 expressing neurons at different pulse durations (1ms, 3ms, 10ms and 25ms). The LASER output powers (mW) for continuous illumination were set on the x-axis. The EP amplitudes were normalized to the 25ms pulse stimulation at 19mW (=1) (y-axis). The average EP amplitudes were plotted against the LASER output powers. Error bars (standard deviations) were put on the graph as well.

Both ChR2 and GtACR2 expressing neurons can already be modulated with pulse durations of 1ms (figures 17 and 18). Pulse durations of 3ms, 10ms and 25ms can also provoke EP (figures 17 and 18). GtACR2 expressing neurons can also be modulated with 1000ms and 2000ms pulses (see addendum figures 41 and 42). The intensity required for modulation differs between the different pulse durations, especially for modulation of ChR2 expressing neurons. Modulation of ChR2 expressing neurons with a pulse duration of 10ms and 25ms is already possible from an output power of 0.3mW. This is in contrast to single pulses of 1ms which need an output power of 2.3mW to modulate ChR2 expressing neurons. Single pulses of 3ms, on the other hand, can sometimes modulate ChR2 expressing neurons with an output power of 0.3mW, but mostly an output power of 2.3mW is required (figure 17). Modulation of GtACR2 expressing neurons is possible from 2.3mW for all different pulse durations (figure 18). EP amplitudes rise with an increasing output power at all pulse durations (figures 17 and 18).

Little difference can be seen on figure 17 between the average EP amplitudes of 3ms, 10ms and 25ms from 6mW to 15mW. A pulse duration of 1ms seems less optimal as stimulation parameter to modulate ChR2 expressing neurons, because the average EP amplitudes are

smaller at each intensity except for 19mW. At 16.5mW and 19mW, a pulse duration of 3ms seems the most efficient to modulate ChR2 expressing neurons (figure 17). Although, 1ms pulses seem less optimal, the error bars (standard deviations) are very big, making 1ms pulses not worse than 3ms, 10ms or 25ms pulses to modulate ChR2 expressing neurons. EP amplitudes of 1ms, 3ms, 10ms and 25ms pulses are comparable for GtACR2 (figure 18). Moreover, pulses of 1000ms and 2000ms seem less optimal to modulate GtACR2 expressing neurons (data not shown). In conclusion, 1ms, 3ms, 10ms and 25ms are all optimal pulse durations for transvascular optogenetic stimulation to modulate ChR2 and GtACR2 expressing neurons.

Furthermore, it was hypothesized that EP durations become longer with prolonged illumination. To determine this, the normalized EP durations of EP were plotted against the pulse durations at different intensities (figures 19 and 20). The normalization was done in the same way as described above for the EP amplitudes.

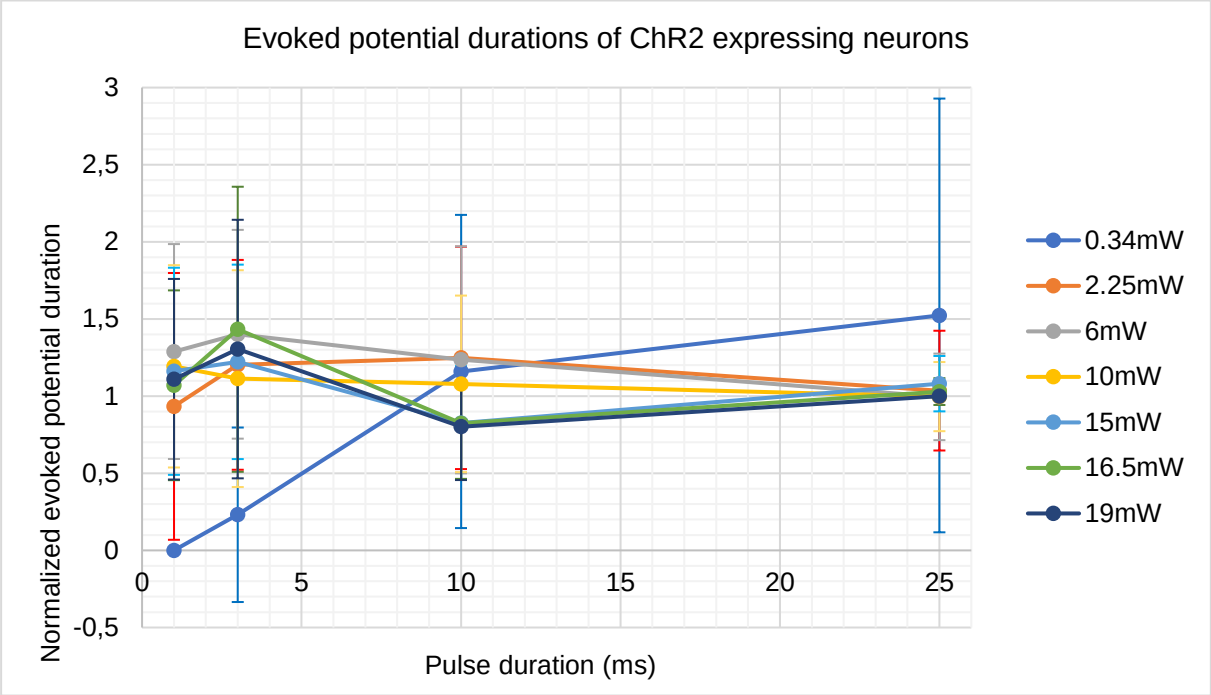

Figure 16: Evoked potential (EP) durations of ChR2 expressing neurons at different LASER output powers (0.3mW, 2.3mW, 6mW, 10mW, 15mW, 16.5mW and 19mW). Pulse durations were set on the x-axis. EP durations were normalized to the 25ms pulse stimulation at 19mW (=1) (y-axis). The average EP durations were plotted against the pulse durations. Error bars (standard deviations) were put on the graph as well.

The above-mentioned hypothesis can be assumed for ChR2 at the lowest intensity (0.3mW). Here, the average EP duration becomes longer with a prolonged illumination time. But the error bars (standard deviations) are very big. However, the average EP durations at all other intensities (2.3mW, 6mW, 10mW, 15mW, 16.5mW and 19mW) remain approximately constant

at short and longer pulse durations with the error bars (standard deviations) taken into account (figure 19).

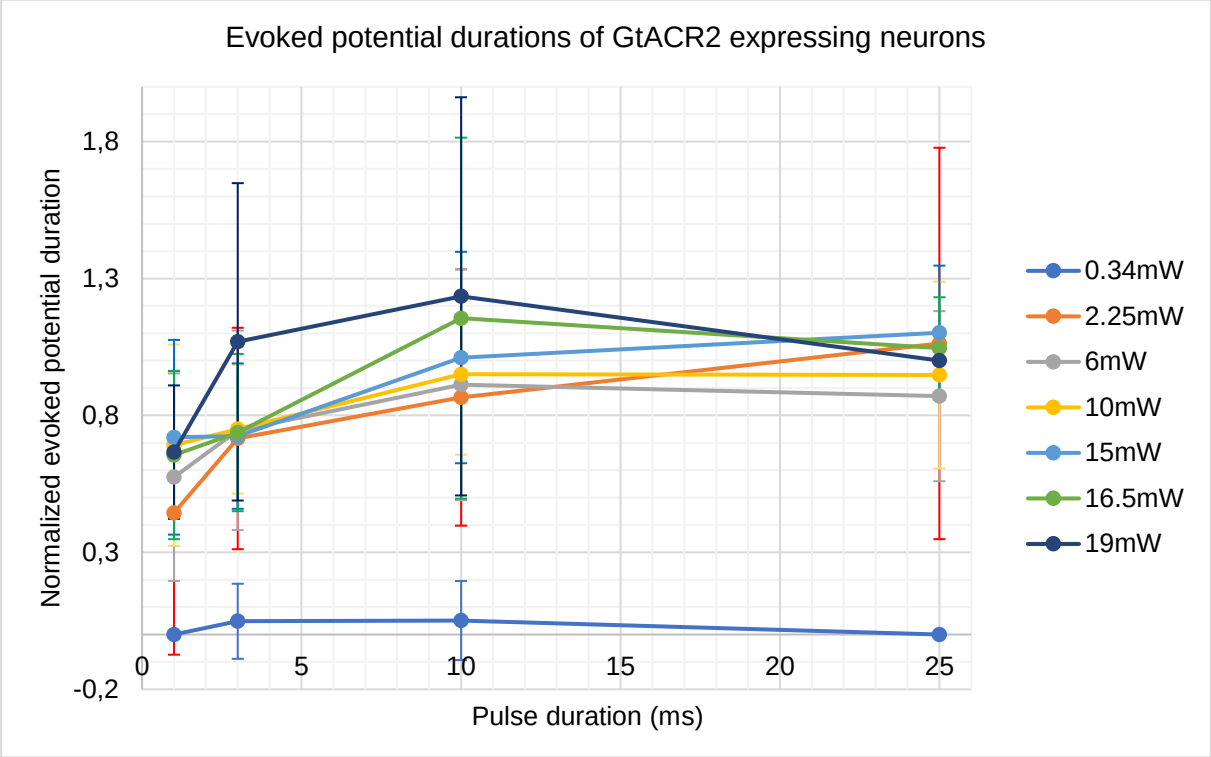

Figure 17: Evoked potential (EP) durations of GtACR2 expressing neurons at different LASER output powers (0.3mW, 2.3mW, 6mW, 10mW, 15mW, 16.5mW and 19mW). Pulse durations were set on the x-axis. EP durations were normalized to the 25ms pulse stimulation at 19mW (=1) (y-axis). The average EP durations were plotted against the pulse durations. Error bars (standard deviations) were put on the graph as well.

Figure 20 shows that EP durations at 0.3mW with 1ms, 3ms, 10ms and 25ms pulses can be neglected. The average EP duration is however longer with 1000ms and 2000ms pulses (data not shown). On top of this, with 1ms, 3ms, 10ms and 25ms pulses at the other intensities a similar trend can be seen: the average EP duration becomes longer up to and including 10ms pulses and then stabilizes. If the error bars are taken into account, little difference can be seen between EP durations with 3ms, 10ms and 25ms pulses (figure 20). EP duration reaches its maximum at 2.3mW with a pulse duration of 1000ms. At 2000ms, however, it is much less long. At 19mW, a declining trend remains visible from 25ms up to 2000ms. At the other intensities, EP duration at 25ms and 1000ms is comparable and again slightly increases at 2000ms (data not shown).

3.3.2 Frequency

To determine if the EP amplitude depends on the stimulation frequency, boxplots of the EP amplitude ratios in response to blue light illumination of 1ms pulses at 18.2mW per frequency

were made for both ChR2 and GtACR2 expressing neurons. Ratios of EP amplitudes were made as follows: the amplitude of the sixth pulse was divided by the amplitude of the first pulse for every measurement at the different stimulation frequencies (figure 21). The boxplots on figure 22 and 23 show that stimulation at lower frequencies cause less attenuation of EP amplitude, both with ChR2 and GtACR2 expressing neurons. Although there is little difference between EP amplitudes of GtACR2 expressing neurons at frequencies of 50Hz and 100Hz (figures 22 and 23).

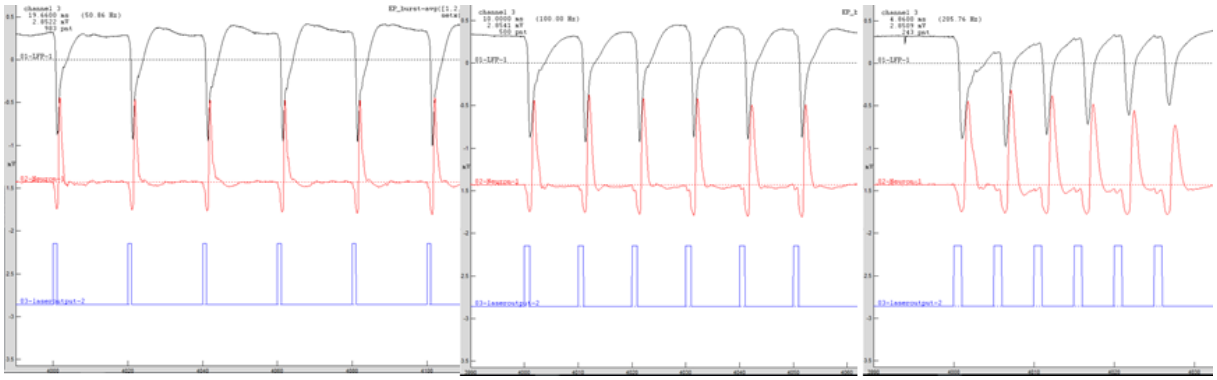

Figure 18: Example of an EP burst measurement of GtACR2 expressing neurons at a depth of 0.6mm under the dura mater at 18.2mW with 1ms pulses at respectively 50Hz, 100Hz and 200Hz from left to right.

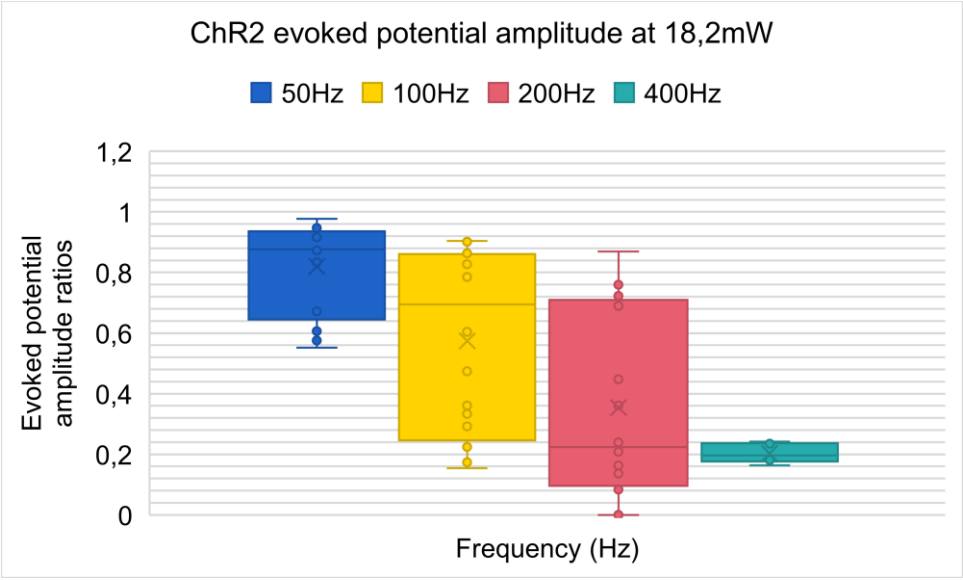

Figure 19: ChR2 evoked potential (EP) amplitudes at 18.2mW at different stimulation frequencies (50Hz, 100Hz, 200Hz and 400Hz). EP amplitudes of the sixth stimulation pulse were divided by EP amplitudes of the first stimulation pulse for every measurement at different frequencies and were plotted on the graph for each stimulation frequency.

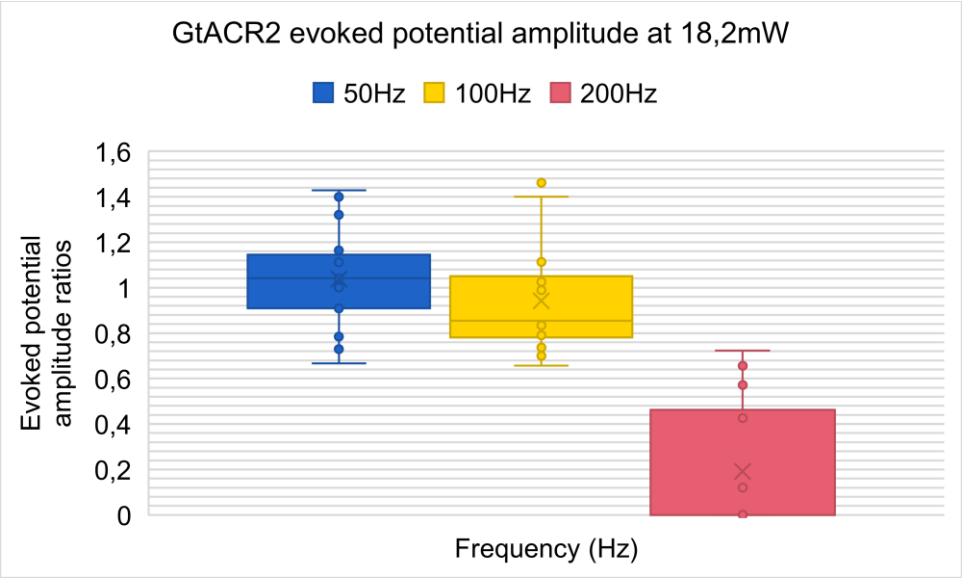

Figure 20: GtACR2 evoked potential (EP) amplitudes at 18.2mW at different stimulation frequencies (50Hz, 100Hz, 200Hz and 400Hz). EP amplitudes of the sixth stimulation pulse were divided by EP amplitudes of the first stimulation pulse for every measurement at different frequencies and were plotted on the graph for each stimulation frequency.

It is known from literature that if it is possible, the use of lower stimulation frequencies is recommended to avoid tissue damage. EP amplitude ratios for all neurons for each stimulation frequency were also plotted against the LASER output powers for 1ms illumination. Output powers for 1ms illumination were used because the graph was made with the data from the IO burst measurements with 1ms pulses (table 1 and figure 24). With this graph it can be determined if the EP amplitudes depend on the output power at different stimulation frequencies (figure 25).

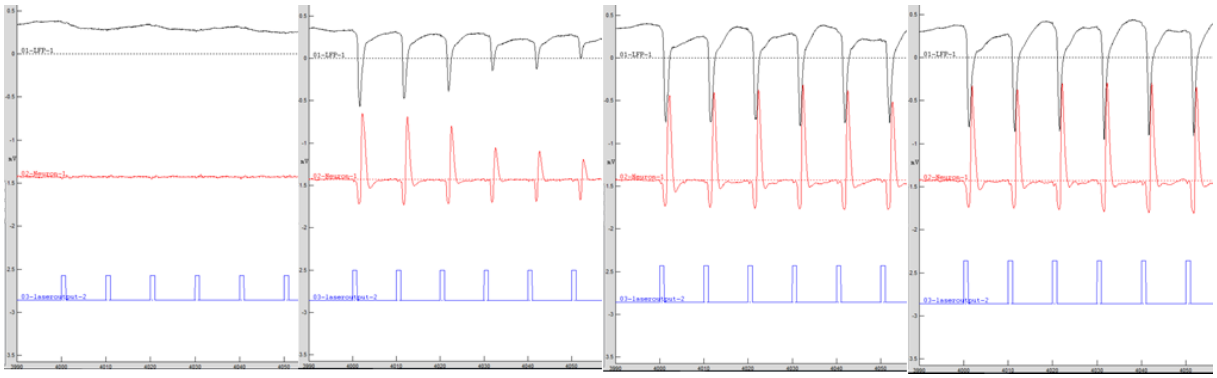

Figure 21:Example of an IO burst measurement of GtACR2 at a depth of 0.6mm under the dura mater at 100Hz with 1ms pulses at 0.2mW - 1.1mW - 3.6mW - 7.3mW respectively from left to right.

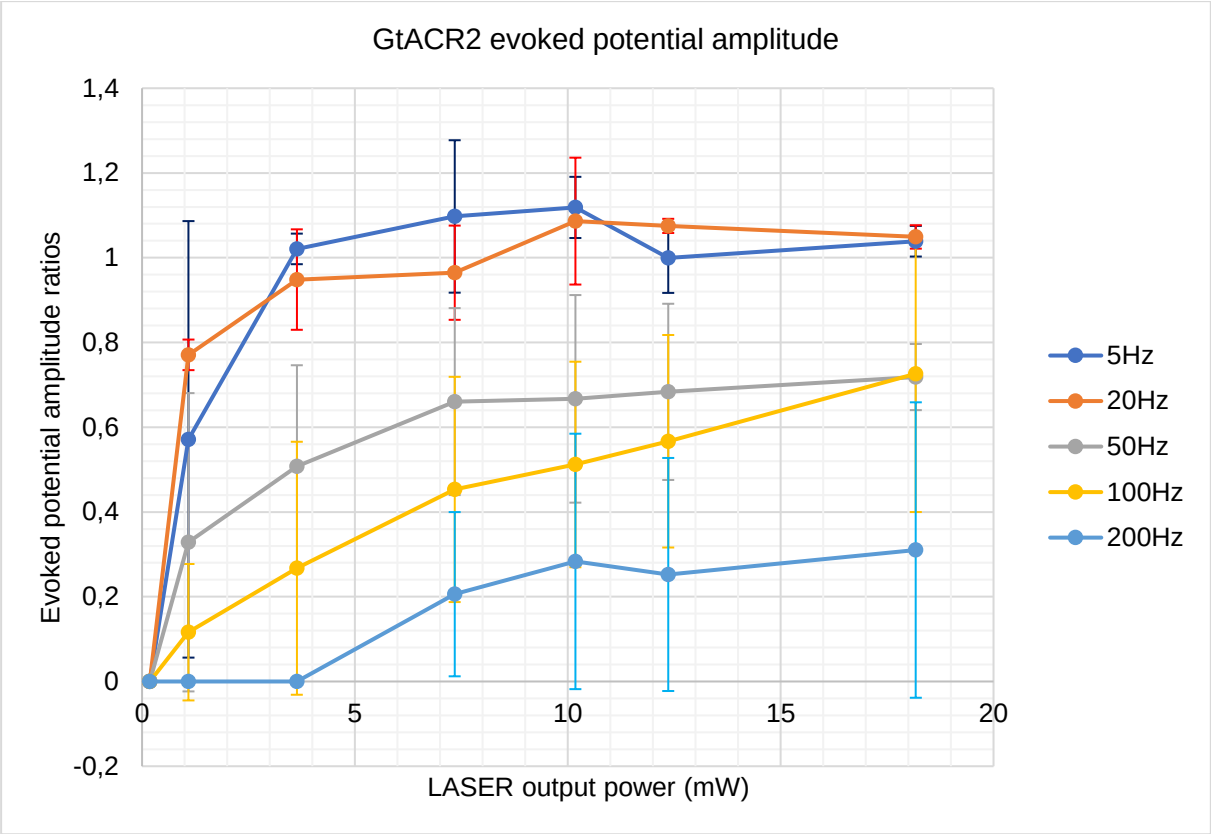

Figure 22: GtACR2 evoked potential (EP) amplitude ratios (y-axis) at different stimulation frequencies (5Hz, 20Hz, 50Hz, 100Hz and 200Hz) in response to different LASER output powers (x-axis). EP amplitudes of the sixth stimulation pulse were divided by EP amplitudes of the first stimulation pulse for every measurement at different frequencies and their averages were plotted on the graph for each stimulation frequency. Errors bars (standard deviations) were also put on the graph.

Figure 25 shows that an output power of 1.1mW is sufficient to evoke EP with GtACR2 expressing neurons at 5Hz, 20Hz, 50Hz and 100Hz. But at 200Hz, an output power of 7.3mW is required to provoke EP. Frequencies of 5Hz and 20Hz are the most optimal stimulation frequencies, because they evoke less attenuated EP. Average EP amplitude ratios rise with an increasing output power for all stimulation frequencies.

Besides IO burst and EP burst measurements at different frequencies, a stimulation protocol of 3' was also applied at different frequencies for GtACR2 expressing neurons, namely 5Hz, 20Hz, 50Hz and 100Hz. During this stimulation protocol, the light was turned on and off according to the following protocol:

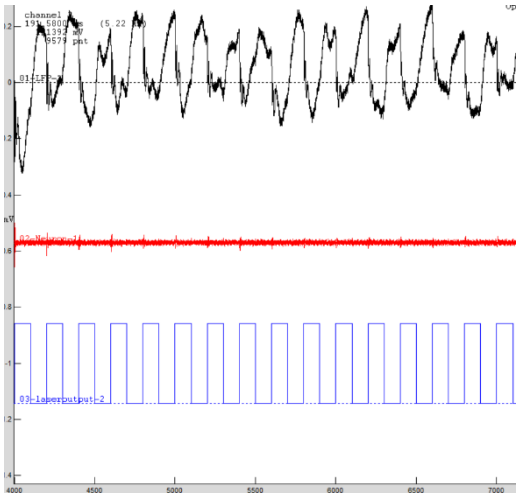

Figure 23: Example of a 3' stimulation protocol for GtACR2 expressing neurons (4" off – 56" on – 4" off – 56" on – 60" off) at a depth of 1.8mm under dura mater. A theta rhythm is induced (black) in response to light stimuli.

4” off – 56” on – 4” off – 56” on – 60” off. A response to stimulation was seen at the highest intensities (19mw – 33.4mW) but not at a lower intensity (~2mW). This specific stimulation protocol also induced a theta rhythm (4-7Hz) on EEG (figure 26).

3.4 INHIBITION OF NEURONAL ACTIVITY

Application of KA increased the activity of cortical neurons, but did not evoke epileptic activity. Stimulation with short light pulses (1ms, 3ms, 10ms and 25ms) did not shown a clear inhibition of neuronal activity. A clear inhibition and also a rebound activation could be demonstrated during prolonged illumination of GtACR2 expressing neurons. The duration of inhibition was qualitatively determined.

Following results were obtained after optical stimulation in one animal. The activity of the cortical neurons could be inhibited with 100ms (at 0.05Hz and 5Hz), 500ms (at 0.05Hz) and 750ms (at 0.05Hz) pulses at 19mW during the recording at a depth of 0.6mm without a rebound activation. Stimulation with 1000ms at the same depth showed full inhibition at 0.1Hz and 0.05Hz during the recording at 19mW. At 0.05Hz, a rebound activation after the stimulation was seen. Furthermore, 28 pulses of 1000ms at 0.5Hz and 19mW were given. The first 10 pulses showed a full inhibition, the other pulses had their own duration of inhibition until the activity of the cortical neurons increased again, namely: 716ms, 680ms, 730ms, 700ms, 680ms, 800ms, 750ms, 770ms, 710ms, 150ms, 690ms, 690ms, 700ms, 180ms, 505ms, 130ms, 410ms and 250ms. Also different intensities were tested of 1000ms pulses at 0.1Hz. Inhibition of the neuronal activity was possible from 2.25mW to 19mW (figure 27). An intensity of 0.34mW had no effect.

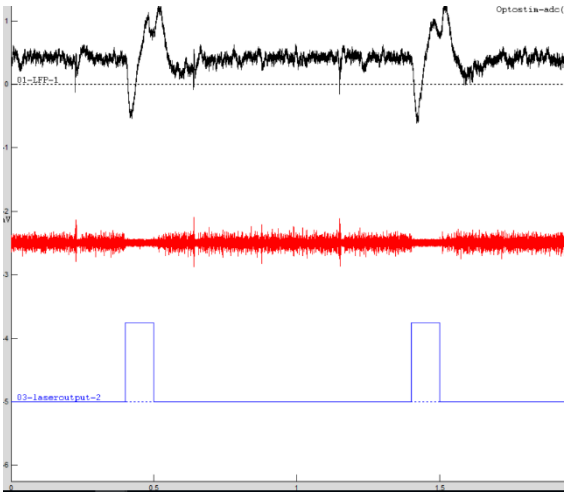

Figure 24: Example of inhibition of neuronal activity with 1000ms pulses at 15mW at a depth of 1.8mm under dura mater.

Measurements in a second animal showed an inhibition from 10mW up to 19mW and 6mW up to 19mW with respectively a 1000ms and 2000ms pulse respectively. In a third animal, 1000ms pulses provoked an inhibition of neuronal activity at 16.5mW at a depth of 1.3mm, 1.4mm and 1.6mm under the dura mater. Both at a depth of 1.6mm and 2.5mm, AP were not inhibited during stimulation from 2.25mW up to 19mW both with a 1000ms and 2000ms pulse. The activity of the cortical neurons could also be inhibited with 2000ms pulses at 0.05Hz and

0.02Hz at a depth of 0.6mm with an intensity of 19mW. When only one pulse of 2000ms at 19mW was given, AP were inhibited until 1445ms after the start of stimulation. Two measurements at 0.1Hz and 19mW showed a full inhibition during the first measurement, but the second showed only a full inhibition during pulse one and two and 575ms of inhibition during the third pulse. Rebound activation after stimulation was demonstrated at all different frequencies except for 0.05Hz with 2000ms pulses at 19mW. Pulses of 4000ms at 0.1Hz showed an inhibition at 2.25mW. When six pulses of 4000ms at 0.05Hz and 19mW were given, an inhibition of 2514ms, 2365ms, 1933ms, 2634ms, 240ms and 0ms was demonstrated. Neuronal activity could also be inhibited with continuous illumination of GtACR2 at 2.25mW. The effect was more long-lasting with a lower intensity compared to a higher intensity.

The 3' stimulation protocol described in section 3.3 was repeated after the application of KA. Occasionally AP could be induced at 5Hz, 20Hz and 50Hz at a low intensity (~2mW). The amplitude of the EP was smaller than with stimulation at higher intensities. AP could not be induced at a low intensity (~2mW) at 100Hz. However, with this intensity, an inhibition could sometimes be detected at 5 Hz, but not at the other frequencies (figure 28). In contrast to lower intensities, AP could always be provoked at the highest intensities (19mW – 33.442mW) in response to stimulation at 5Hz and 20Hz. Furthermore, stimulation at 50Hz and 100Hz sometimes evoked EP, both in the beginning and middle of stimulation, but with a small amplitude. An inhibition could be seen at 5Hz stimulation at the highest intensity. Occasionally inhibition could also be demonstrated at 20Hz, 50Hz and 100Hz.

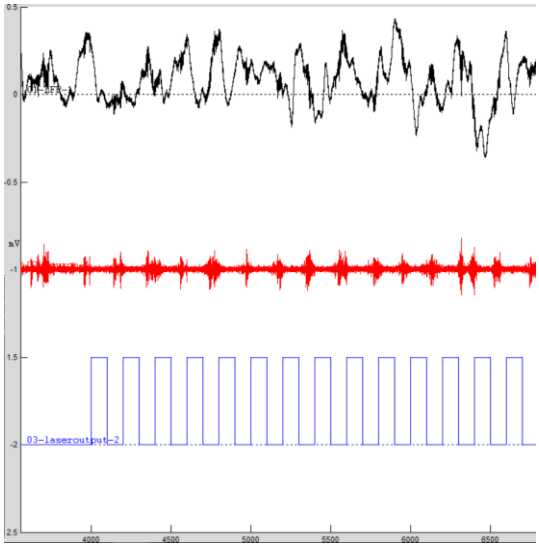

Figure 25: Example of a 3' stimulation at 5Hz and ~2mW at a depth of 1.8mm under dura mater.

3.5 HISTOLOGY

The cortical expression of both ChR2 and GtACR2 under a CamKIIα promotor coupled respectively to GFP and mCherry was verified through an immunofluorescence staining and visualized with a fluorescence microscope (4x magnification)(figures 29 and 30).

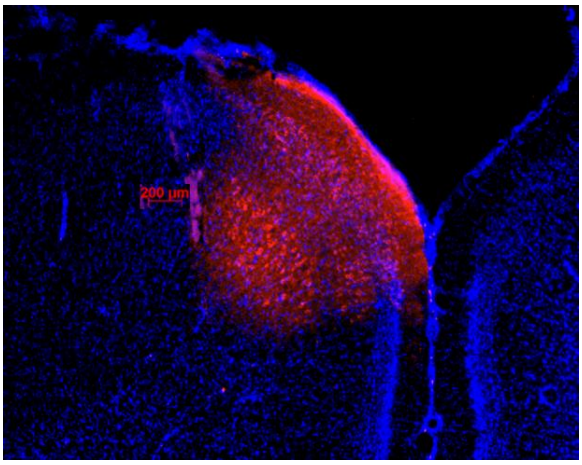

Figure 26: DAPI (blue) and GtACR2-mCherry (red) expression.

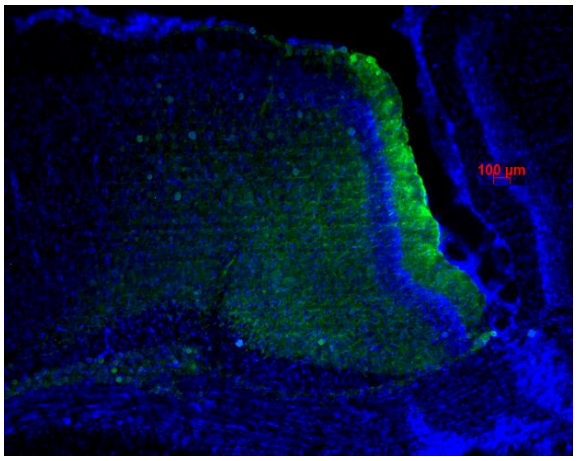

Figure 27: DAPI (blue) and ChR2-GFP (green) expression.

Opsin expression stayed unilaterally and did not spread to the other side of the cortex. Also, opsin expression was very focal around the injection sites (figures 29 and 30).

The expression area and spatial extent of the expression of both ChR2 and GtACR2 were measured (table 3). The average expression volume is 1.3mm^3 for ChR2 expressing cortical tissue and 2,3mm^3 for GtACR2 expressing cortical tissue.

ChR2	**Area of expression (mm^2)**			**GtACR2**	**Area of expression (mm^2)**					
	Rat 1	Rat 2	Rat 3		Rat 4	Rat 5	Rat 6	Rat 7	Rat 8	Rat 9
Slice 1	0	0	0	Slice 1	1	1	3,2	0,38	0	0
Slice 2	0	0,8	2	Slice 2	1,5	1	3,9	0,4	2,6	1,6
Slice 3	0	1,4	3,4	Slice 3	1,6	1,8	4,1	1,8	3	2,2
Slice 4	2,9	3	4,4	Slice 4	1,7	4,2	4,8	3,1	1,5	3,5
Slice 5	0,09	1,9	3	Slice 5	1,6	3,7	4,7	2,2	1,1	1,6
Slice 6	0	1,1	2	Slice 6	1,6	3	4,3	0,75	0,3	1,5
Slice 7	0	0	0	Slice 7	1,4	0	4,3	0,5	0,3	0,8
	Volume of expression (mm^3)				**Volume of expression (mm^3)**					
	0,5836	1,16	2,256		1,848	2,268	5,092	1,33	1,52	1,68
Average	1,3332			Average	2,289666667					

Table 3: Expression area and volume of ChR2 and GtACR2 expressing cortical tissue.

In the below-mentioned table, the results of the GFP/NeuN double staining are summarized. The number of double positive cells are very low. Mostly the ratio of double positive cells is also negligible, and because of this one cannot speak of colocalization (table 4 and figure 31).

Number of cell bodies	70	92	122	20	38	0	13	33	27	61	58	25	7	15	9
Double positive cells	6	2	2	1	8	0	0	2	0	11	1	0	0	1	0
Ratio of double positive cells	9%	2%	2%	5%	21%	0%	0%	6%	0%	18%	2%	0%	0%	7%	0%

Table 4: Number of cell bodies, amount of double positive cells and ratio of double positive cells in GFP/NeuN double staining.

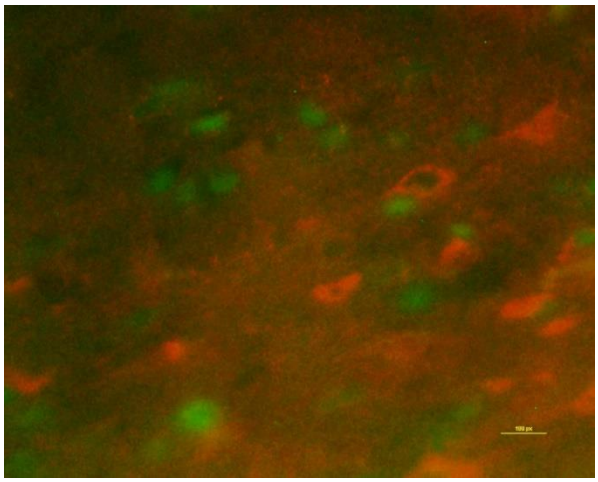

Figure 28: mCherry (red)/NeuN (green) double staining.

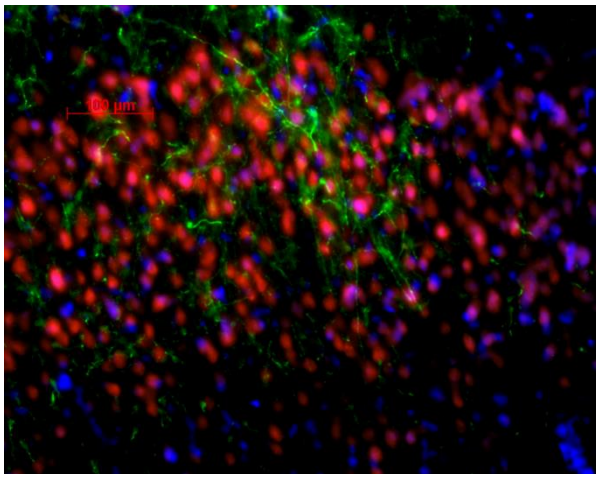

Figure 29: GFP (green)/NeuN (red) double staining and DAPI (blue).

It was not possible to take pictures with the Carl Zeiss, Axiovert 200M microscope of the mCherry/NeuN double staining, because the green color of the NeuN could not be visualized. Because of this, pictures of this double staining were taken with the Nikon Eclipse TE2000-E microscope. These pictures were of poor quality, so quantification of cell bodies and double positive cells was not possible. After merging NeuN and mCherry pictures with Fiji, colocalization was seen, but a confocal microscope is required to visualize this better (figure 32).

Furthermore, the immunofluorescence staining with VGluT1 was optimized. The expression of the 1/1000, 1/2000, 1/5000 dilutions of the goat VGluT1 primary antibody could be visualized. The other dilutions: 1/7500, 1/10000 and 1/15000 are still being investigated.

4 DISCUSSION

This study investigated whether transvascular optogenetic stimulation with blue light with an optic fiber placed against the ipsilateral wall of the SSS is possible. This turned out to be the case. Furthermore, the maximal distance at which modulation of ChR2 and GtACR2 expressing neurons is still possible was determined. Transvascular optogenetic modulation of ChR2 and GtACR2 expressing neurons is respectively possible up to a depth of 1.5-2.5mm and 1.9-2.1mm under the dura mater and up to 0.9-1.3mm and 0.6-0.9mm lateral to the edge of the SSS. On top of this, the optimal stimulation parameters, namely required power, pulse duration and stimulation frequency, for transvascular optogenetic stimulation were determined. A power of 0.3mW was sufficient for 10ms and 25ms pulses, 0.3-2.3mW for 3ms pulses and 2.3mW for 1ms pulses for ChR2 expressing neurons. A power of 2.3mW for all pulse durations for GtACR2 expressing neurons appeared to be sufficient. EP amplitudes raised with an increasing output power at 1ms, 3ms, 10ms and 25ms pulses. All these pulse durations seemed optimal for transvascular optogenetic stimulation to modulate opsin expressing neurons. Stimulation at lower frequencies (5Hz, 20Hz and 50Hz) resulted in less attenuation of EP amplitude with both opsins compared to higher frequencies (100Hz, 200Hz and 400Hz), and are thus the most optimal stimulation frequencies. After application of KA, neuronal activity could be inhibited during prolonged illumination of GtACR2.

4.1 MAXIMAL DISTANCE

Transvascular optogenetic modulation of ChR2 expressing neurons was possible up to a depth of 1.5-2.5mm under the dura mater and up to 0.9-1.3mm lateral to the edge of the SSS in this study with a 60µm diameter optic fiber placed into the SSS with a maximal intensity of 67.9mW/mm^2. This intensity was calculated as followed: 19mW/0.28mm^2, with 0.28mm^2 the area of the light cone spread out of the optic fiber (radius= 30µm). In comparison with this study, Foutz TJ et. al predicted a modulation of ChR2 expressing neurons up to 1.3mm from a 0.2mm diameter optic fiber with an intensity of 380mW/mm^2 during stimulation with a 5ms pulse [26]. Aravanis et. al estimated a modulation of ChR2 expressing neurons up to 1.4mm depth in the rat motor cortex using the same stimulation parameters [18]. Modulation of ChR2 expressing neurons in a non-human primate cortex was possible up to 1mm from an optic fiber tip with an intensity of 80mW/mm^2 [44]. On top of these findings, it was also reported that illumination is effective up to a depth of 1.5mm without brain tissue damage with a 0.2mm diameter optic fiber [12].

Transvascular optogenetic modulation of GtACR2 expressing neurons was possible up to a depth of 1.9-2.1mm under the dura mater and up to 0.6-0.9mm lateral to the edge of the SSS in this study with a maximal intensity of 67.9mW/mm^2 with a 60µm diameter optic fiber placed into the SSS, which is comparable to the results for ChR2. Instead of investigating the maximal distance at which GtACR2 expressing neurons can be modulated, Mathias Mahn et. al revealed that stimulation of GtACR2 with 480nm light provides optimal inhibition of neuronal activity at 0.5mm distance from the optic fiber tip [35]. No other studies were found who investigated the maximal distance at which GtACR2 expressing neurons can still be modulated.

From literature research and above-mentioned results, it can be concluded that modulation of ChR2 and GtACR2 expressing neurons was possible up to great distance in this study. Moreover, LASER light is neither more absorbed by the SSS than the brain itself. Thus, transvascular optogenetic stimulation is as efficient as the intraparenchymatic optogenetic stimulation to activate opsins at a certain distance.

4.2 OPTIMAL STIMULATION PARAMETERS

Although AP were not provoked in this experiment in response to stimulation of ChR2 expressing neurons, this should normally be the case. On top of this, it is known that single unit activity can be recorded too. Probably we have not succeeded in getting the electrode close enough to the neurons to measure AP and single unit activity.

4.2.1 Output power and pulse duration

Zhang et. al stated that a light intensity of 5-12mW/mm^2 is required to modulate ChR2 expressing neurons [32]. In contrast, Aravanis et. al found that a minimal blue light intensity of 1mW/mm^2 is required for generation of ChR2 evoked AP and that robust spiking is achieved with a blue light intensity of 10mW/mm^2 [18]. In accordance to Zhang et al, Diester et. al reported that ChR2 expressing neurons could be modulated with an intensity of 0.5-20mW/mm^2 at the recording site, which corresponds to an intensity of 5-200mW/mm^2 at the optic fiber tip [12, 45].

Pulse duration is, in addition to LASER output power, an important parameter to modulate ChR2 expressing neurons [26]. Foutz TJ et al. discovered that short pulse durations require larger LASER output powers compared to longer pulse durations to modulate ChR2 expressing neurons [26]. This could be confirmed by this study. A LASER output power of 0.3mW (1.1mW/mm^2) was already sufficient to modulate ChR2 expressing neurons with 10ms

and 25ms pulses, but a LASER output power of 0.3-2.3mW (1.1-8.2mW/mm^2) and 2.3mW (8.2mW/mm^2) were required to modulate ChR2 expressing neurons respectively with 3ms and 1ms pulses.

The threshold to modulate ChR2 expressing neurons depends on pulse duration, ion channel density and ion channel conductance. A higher ion channel density and conductance results in a lower modulation threshold. A decreased light absorption, scattering, optic fiber-to-stimulated-neuron distance and NA are also correlated with a lower modulation threshold [26]. In this study, there was no correlation between the optic fiber-to-stimulated-neuron distance and modulation threshold (see section 3.3.1).

GtACR2 expressing neurons could be modulated in this study with a LASER output power of 2.3mW (8.2mW/mm^2) at all pulse durations. Malyshev AY et. al found that pulses of 10ms can induce AP in GtACR2 expressing neurons [28]. Mathias Mahn et. al showed a significant reduction in neuronal activity *in vivo* upon 5s illumination/activation of GtACR2 with 460nm light of 0.5-1mW/mm^2 at the recording site [35].

In conclusion, the required powers and pulse durations for modulation in this study are comparable to the powers and pulse durations found in literature.

4.2.2 Frequency

Neurons expressing ChR2 are able to follow stimulation frequencies of 5Hz, 10Hz and 20Hz with 10ms pulses. Moreover, spikes are generated by these neurons every light stimulus [3, 20]. It is also known from literature that ChR2 can drive reliable AP trains up to 50Hz [32]. This could also be demonstrated in this study with 1ms pulses at 50Hz. On top of this, lower frequencies provoked less attenuated EP at 18.2mW for both ChR2 and GtACR2 expressing neurons with 1ms pulses, but also at different intensities for GtACR2.

Reliable spike trains were also generated at 100Hz stimulation for both ChR2 and GtACR2 expressing neurons, but not at 200Hz and 400Hz stimulation with 1ms pulses. This is in accordance Foutz TJ et. al's study, which demonstrated the reliable response of neurons to a stimulation frequency of 90Hz with 5ms pulses using a high light intensity [26]. A big difference was seen between EP amplitudes of ChR2 expressing neurons at 50Hz and 100Hz, although there was little difference between EP amplitudes of GtACR2 expressing neurons at 50Hz and 100Hz. It was hypothesized that the ability of neurons to follow high frequency stimulation depends on neuronal cell type and difference in kinetics of the ion channel that is being stimulated. Both Zhang et. al and Cardin JA et. al stated that the ability to follow a high

optogenetic stimulation frequency mainly depends on the ChR2 expressing cell type [20, 32]. For example, dentate gyrus hilar interneurons are able to follow higher frequencies in comparison with pyramidal neurons. This ability also depends on LASER output power and pulse duration, but less on kinetics of ChR2 [32]. On top of this, the ion channel density in the opsin expressing tissue has also an impact on the ability to follow high frequency stimulation. Reliable spike trains can be generated up to 100Hz stimulation with an increased channel density, but with a decreased channel density, AP generation in response to every light pulse was possible up to 30Hz [26].

5Hz and 20Hz stimulation with 1ms pulses provoked less attenuated EP for GtACR2 expressing neurons and are thus the most optimal stimulation frequencies to modulate GtACR2 expressing neurons. Malyshev AY et. al found that GtACR2 can drive reliable AP trains of up to 10Hz with short light stimuli. 15-20Hz stimulation can also induce reliable AP trains in the beginning of stimulation, but further in stimulation, these frequencies induce subthreshold PSP. If the stimulation frequency is too high, generation of AP trains does not occur [28].

4.3 INHIBITION OF NEURONAL ACTIVITY

In this study, KA was applied to increase the activity of cortical neurons. Normally, KA, which is a L-glutamate analogue, is used to model TLE. If KA is applied into the brain, it preferentially targets the hippocampus, alters cortical excitability and induces neuronal depolarisation and seizures [7, 46]. This is in contrast with this study where KA did not induce epilepsy, but only increased neuronal activity in the cortex.

Optogenetics had already been shown to be effective to reduce and delay the time of onset of epileptic seizures *in vivo* and *in vitro* using NpHR and yellow light guided by an optic fiber placed into the hippocampus [15, 17]. Reduction of seizures with NpHR under a CaMKIIα promotor expressed in the hippocampus could be shown in the rat lithium pilocarpine model [15], KA mouse model for TLE [47], when expressed in the motor cortex in the tetanus toxin rat model [48], etc. [3]. Optogenetics using GtACR2 had also been shown effective to inhibit behaviour in fruit flies and larval zebrafish [36, 49, 50].

However, optogenetic inhibition had never been tried with an intravascular optic fiber and GtACR2 expressed in the cortex under a CaMKIIα promotor. Increased cortical activity could be inhibited during prolonged illumination of GtACR2 during this study. This inhibition was observed between 2.3mW (8.2mW/mm^2) and 19mW (67.9mW/mm^2). An intensity between 0.3mW (1.1mW/mm^2) and 2.3mW (8.2mW/mm^2) decreased the cortical activity but no full

inhibition was seen. On top of this, an intensity of 0.3mW (1.1mW/mm^2) had no effect. This is in contrast with the studies of Govorunova EG et. Al and Mathias Mahn et. al, which found that spiking can be precisely suppressed in GtACR2 expressing neurons with a blue light intensity of 0.005mW/mm^2 and 0.5-1mW/mm^2 respectively [27, 35].

Although an inhibition of neuronal activity could be demonstrated, a rebound electrophysiological activity was seen after illumination of GtACR2. This can be due to an increased intracellular Cl^- concentration or decreased intracellular H^+ concentration, which can trigger Cl^- efflux or H^+ influx causing depolarization [13, 50]. This is in contrast to NpHR. No rebound electrophysiological activity was seen after illumination of NpHR in the study of Sukhotinsky I et. al [15]. However, Tonnesen J et. al demonstrated an increase in spontaneous activity after NpHR activation with light. But, this increase was the same in NpHR transduced and non-transduced tissue, which indicates that NpHR does not cause this rebound activity after illumination [17].

Cl^- regulation affects brain function by dictating the $GABA_A$ receptor reversal potential. The $GABA_A$ receptor is an inhibitory ionotropic ligand-gated neurotransmitter receptor that carry Cl^- ions, which equilibrium potential is close to the resting potential (-70mV). Its reversal potential influences neuronal excitability [51]. Intracellular Cl^- accumulation can cause a shift in $GABA_A$ receptor reversal potential in pyramidal neurons from hyperpolarization towards depolarization, which can increase activation of neurons and promote epileptic activity [12, 15, 17, 48, 50]. This could explain EP generated in response to a single light pulse [6]. Although NpHR activation results in a Cl^- influx, NpHR does not shift the $GABA_A$ receptor reversal potential in pyramidal neurons, because endogenous Cl^- pumps, such as KCC2, are able to pump the excess amount of Cl^- ions out of the soma and normalize the potential [12, 15, 17, 35]. Raimondo et. al stated that effects on the $GABA_A$ receptor reversal potential are related to the size and duration of the Cl^- photocurrent. NpHR with small photocurrents do not cause a shift in the $GABA_A$ receptor reversal potential while NpHR with larger photocurrents do cause a shift. Unlike NpHR with larger photocurrents and GtACR2, Arch never cause a shift in the $GABA_A$ receptor reversal potential [52].

Normally, the cytoplasmic and somatic Cl^- concentration are low in neurons (respectively 7mM intracellularly and 120mM extracellularly [11]). In contrast to the soma, Cl^- concentration in axons is higher due to an absence of the KCC2 pump [35]. The equilibrium potential of Cl^- is -76mV [11].

The action of GtACR2 depends on the Cl^- gradient [13]. If GtACR2 is illuminated with blue light, it generates hyperpolarizing currents through an influx of Cl^- in the soma at E_h above the Nernst

equilibrium potential for Cl^- [13, 27]. In this way, GtACR2 is a strong cell silencer [28]. In axons, a high Cl^- concentration leads to a depolarisation and AP, which propagate retrogradely to the soma, through an efflux of Cl^- ions because of a depolarizing Cl^- reversal potential [13, 28]. This makes GtACR2 also a cell activator on top of a cell silencer [28].
Prolonged illumination (>100ms) of GtACR2 in the soma causes a hyperpolarization and thus an inhibition of the neuronal activity and also one spike at the beginning of stimulation [28], which could also be demonstrated in this study. This hyperpolarization is stronger than the depolarization induced by GtACR2 activation in the axons [28].

Mathias Mahn et. al overcame depolarization at axon terminals by designing a soma-targeted GtACR2 (stGtACR2). This tool has increased membrane targeting and photocurrents, a high light sensitivity, fast kinetics, decreased axonal excitation and thus reduced antidromic AP, allowing efficient inhibition of neuronal activity [35].

In this study, inhibition of neuronal activity was limited to inhibiting excitatory pyramidal neurons. Although the selectivity of the used CamKIIα promotor for excitatory glutamatergic neurons has been demonstrated, it is possible that GtACR2 was non-specifically expressed in inhibitory neurons. Stimulation of GtACR2 in inhibitory neurons would cause silencing of inhibitory neurons, resulting in epileptic activity [15]. To rule out this non-specific expression, a double staining is required (see section 4.4).

4.4 HISTOLOGY

The average expression volume was $1.3mm^3$ for ChR2 expressing cortical tissue and $2,3mm^3$ for GtACR2 expressing cortical tissue in this study. The expression volume depends on the type of viral vector, method of injection and quantity of viral particles injected [18, 32].

Aravanis et. al states that the expression volume for ChR2 is often $<1mm^3$. However, Aravanis et. al used a high titer lentivirus ($>10^9$ gc/ml) to transduce the neurons with ChR2 [18]. This is in contrast to this study, where a high titer AAV was used.

Colocalization could be seen with both the NeuN/GFP and NeuN/mCherry double staining performed in this study, but a confocal microscopy is required to better visualize colocalization. NeuN is a neuronal marker which colors the nucleus. GFP and mCherry color the neuronal membrane. Because of this, it was difficult to see colocalization. The staining for VGluT1 is still being optimized. VGluT1 targets the neuronal membrane of glutamatergic neurons, which makes it better for visualizing colocalization with GFP and mCherry. If this staining is optimized, it could be used to verify if ChR2 and GtACR2 were expressed specifically in the excitatory

cortical pyramidal neurons as hypothesized from our use of the glutamatergic, neuron-specific, CaMKII*α* promoter to drive ChR2 and GtACR2 expression. Therefore, antibodies for either CaMKII*α* or glutamate decarboxylase-67(GAD67), which is a GABA-producing enzyme that is specifically expressed in inhibitory interneurons, could be used [3].

4.5 ANAESTHESIA

During transvascular optogenetic stimulation, anaesthesia was set on 1.5% isoflurane instead of 2% isoflurane if possible, because it is known from literature that the effects of optogenetic stimulation on LFP signals and AP generation vary with anaesthesia depth [20]. It has even been shown that excitatory PSP are depressed by isoflurane anaesthesia [6]. Neuronal excitability also differs between *in vitro* slices, anaesthetized animals and awake animals [13]. Because of this, there is no certainty that modulation of neuronal activity *in vivo* works similar in awake animals.

4.6 FUTURE PERSPECTIVES

This study gave a first impression of transvascular optogenetic stimulation and its optimal stimulation parameters, but further research is necessary to specify and confirm these parameters. Simultaneous functional magnetic resonance imaging during optogenetic stimulation can be used to determine the efficacy of light delivery and stimulation but also opsin expression in brain tissue [12].

Since the effectiveness of optogenetics has already been proven in numerous *in vitro* and preclinical studies (mostly in rodents) (see section 4.3) with NpHR, but also with GtACR2 *in vitro,* in fruit flies and larval zebrafish, but not yet in mammals, it is also necessary to further investigate the possible anti-epileptic effects of neuronal inhibition with GtACR2 in mammals.

In the distant future, one could think of translating (transvascular) optogenetics to humans. Clinical trials, which imply AAV delivery to human brains, have already been carried out for Parkinson's disease and Alzheimer's disease [3]. In contrast to this study, no opsins were built into these AAV. Expression of a large number of opsins in brain tissue could result in physiological differences and an altered function of cells [29]. On top of this, most optogenetic studies were performed in rodents, which have a small brain compared to humans [12]. For these reasons, it is necessary to be careful and do extra research after use of opsins in the human brain before translating optogenetics to humans [29].

Advantages of optogenetics compared to other epilepsy treatments are strong temporal and spatial precision and cell-specific mechanism of action (see section 1.1). But before one could translate this technique to humans, some physiological problems first need to be overcome. The rebound electrophysiological activity which was seen after illumination of GtACR2 needs to be avoided, because this can lead to an increased excitability of neurons. But also the depolarization at axon terminals leading to antidromic AP and activation of neuronal cell bodies need to be overcome. StGtACR2 have been shown to offer a solution (see section 4.3)[35].

Furthermore, some practical problems arise which need to be overcome before translation to humans will become possible. Miniaturization of light sources without power loss, development of feedback-closed-loop systems, optimizing light coverage of larger brain structures and light penetration through brain tissue are some examples of these practical problems [12].

5 CONCLUSION

This dissertation showed the possibility of transvascular optogenetic stimulation with blue light transmitted by an optic fiber placed against the ipsilateral wall of the SSS. Based on the stimulation protocols carried out with the microelectrode placed at different depths and distances from the optic fiber tip in the SSS, it could also been demonstrated that EP amplitudes, if provoked and not felt out, in response to blue light stimulation do not depend on depth and distance from the optic fiber tip. Transvascular optogenetic modulation of ChR2 and GtACR2 expressing neurons is respectively possible up to a depth of 1.5-2.5mm and 1.9-2.1mm under the dura mater and up to 0.9-1.3mm and 0.6-0.9mm lateral to the edge of the SSS, making transvascular optogenetics as efficient as intraparenchymatic optogenetic stimulation to modulate neurons expressing opsins at a certain distance. Furthermore the optimal stimulation parameters, namely required power, pulse duration and stimulation frequency for transvascular optogenetic stimulation to modulate ChR2 and GtACR2 expressing neurons were determined. A power of 0.3mW was sufficient for 10ms and 25ms pulses, 0.3mW-2.3mW for 3ms pulses and 2.3mW for 1ms pulses was required, confirming that larger LASER output powers are needed for shorter pulse durations to modulate ChR2 expressing neurons. To modulate GtACR2 expressing neurons, 2.3mW at all pulse durations appeared to be sufficient. EP amplitudes raised with an increasing output power at 1ms, 3ms, 10ms and 25ms pulses. All these pulse durations seemed optimal for transvascular optogenetic stimulation to modulate neurons expressing both opsins. Stimulation at lower frequencies (5Hz, 20Hz and 50Hz) caused less attenuation of EP amplitude, with both opsins, and are thus the most optimal stimulation frequencies. After application of KA, neuronal activity could be clearly inhibited during prolonged illumination of GtACR2. The results of the histological analysis showed an unilateral and focal expression for both opsins, with an average expression volume of 1.3mm^3 for ChR2 expressing cortical tissue and 2,3mm^3 for GtACR2 expressing cortical tissue. Confocal microscopy is necessary to better visualize colocalization after GFP/NeuN and mCherry/NeuN double stainings.

Although this dissertation gave a first impression of transvascular optogenetic stimulation and its optimal stimulation parameters, further research is still necessary to confirm and further specify these parameters and to further investigate the possible anti-epileptic effects of neuronal inhibition with GtACR2 or more specifically stGtACR2.

6 REFERENCES

1. Pieter van Mierlo WS, Evelien Carrette, Alfred Meurs, Dirk Van Roost, Paul Boon and Kristl Vonck (2015) Lokalisatie van de epileptische focus op basis van netwerkanalyse van hersensignalen. *NEURON (NEDERLANDSE ED)* **20**: 8-12
2. Zhao M, Alleva R, Ma H, Daniel AG, Schwartz TH (2015) Optogenetic tools for modulating and probing the epileptic network. *Epilepsy Res* **116**: 15-26
3. Tung JK, Berglund K, Gross RE (2016) Optogenetic Approaches for Controlling Seizure Activity. *Brain Stimul* **9**: 801-810
4. Bromfield EB CJ, Sirven JI (2006) *An Introduction to Epilepsy*.
5. Bernstein JG, Han X, Henninger MA, Ko EY, Qian X, Franzesi GT, McConnell JP, Stern P, Desimone R, Boyden ES (2008) Prosthetic systems for therapeutic optical activation and silencing of genetically-targeted neurons. *Proc SPIE Int Soc Opt Eng* **6854**: 68540H
6. Chiang CC, Ladas TP, Gonzalez-Reyes LE, Durand DM (2014) Seizure suppression by high frequency optogenetic stimulation using in vitro and in vivo animal models of epilepsy. *Brain Stimul* **7**: 890-9
7. Osawa S, Iwasaki M, Hosaka R, Matsuzaka Y, Tomita H, Ishizuka T, Sugano E, Okumura E, Yawo H, Nakasato N*, et al.* (2013) Optogenetically Induced Seizure and the Longitudinal Hippocampal Network Dynamics. *Plos One* **8**
8. Vonck K (2017-2018) *Klinische Neurologie*.
9. Berg AT, Berkovic SF, Brodie MJ, Buchhalter J, Cross JH, van Emde Boas W, Engel J, French J, Glauser TA, Mathern GW*, et al.* (2010) Revised terminology and concepts for organization of seizures and epilepsies: report of the ILAE Commission on Classification and Terminology, 2005-2009. *Epilepsia* **51**: 676-85
10. Graves TD (2006) Ion channels and epilepsy. *QJM* **99**: 201-17
11. Raedt R (2016-2017) *Neurobiologie*.
12. Kokaia M, Andersson M, Ledri M (2013) An optogenetic approach in epilepsy. *Neuropharmacology* **69**: 89-95
13. Wiegert JS, Mahn M, Prigge M, Printz Y, Yizhar O (2017) Silencing Neurons: Tools, Applications, and Experimental Constraints. *Neuron* **95**: 504-529
14. Kwan P, Brodie MJ (2000) Early identification of refractory epilepsy. *N Engl J Med* **342**: 314-9
15. Sukhotinsky I, Chan AM, Ahmed OJ, Rao VR, Gradinaru V, Ramakrishnan C, Deisseroth K, Majewska AK, Cash SS (2013) Optogenetic Delay of Status Epilepticus Onset in an In Vivo Rodent Epilepsy Model. *Plos One* **8**
16. Zhang F, Gradinaru V, Adamantidis AR, Durand R, Airan RD, de Lecea L, Deisseroth K (2010) Optogenetic interrogation of neural circuits: technology for probing mammalian brain structures. *Nat Protoc* **5**: 439-56
17. Tonnesen J, Sorensen AT, Deisseroth K, Lundberg C, Kokaia M (2009) Optogenetic control of epileptiform activity. *P Natl Acad Sci USA* **106**: 12162-12167
18. Aravanis AM, Wang LP, Zhang F, Meltzer LA, Mogri MZ, Schneider MB, Deisseroth K (2007) An optical neural interface: in vivo control of rodent motor cortex with integrated fiberoptic and optogenetic technology. *J Neural Eng* **4**: S143-56
19. Sidor MM, Davidson TJ, Tye KM, Warden MR, Diesseroth K, McClung CA (2015) In vivo optogenetic stimulation of the rodent central nervous system. *J Vis Exp*: 51483
20. Cardin JA, Carlen M, Meletis K, Knoblich U, Zhang F, Deisseroth K, Tsai LH, Moore CI (2010) Targeted optogenetic stimulation and recording of neurons in vivo using cell-type-specific expression of Channelrhodopsin-2. *Nat Protoc* **5**: 247-254
21. Forcelli PA (2017) Applications of optogenetic and chemogenetic methods to seizure circuits: Where to go next? *J Neurosci Res* **95**: 2345-2356
22. Gomez JL, Bonaventura J, Lesniak W, Mathews WB, Sysa-Shah P, Rodriguez LA, Ellis RJ, Richie CT, Harvey BK, Dannals RF*, et al.* (2017) Chemogenetics revealed: DREADD occupancy and activation via converted clozapine. *Science* **357**: 503-507
23. Govorunova EG, Koppel LA (2016) The Road to Optogenetics: Microbial Rhodopsins. *Biochemistry (Mosc)* **81**: 928-40
24. Dolgikh DA, Malyshev AY, Roshchin MV, Smirnova GR, Nekrasova OV, Petrovskaya LE, Feldman TB, Balaban PM, Kirpichnikov MP, Ostrovsky MA (2016) Comparative characteristics

of two anion-channel rhodopsins and prospects of their use in optogenetics. *Dokl Biochem Biophys* **471**: 440-442
25. Paz JT, Huguenard JR (2015) Optogenetics and Epilepsy: Past, Present and Future. *Epilepsy Curr* **15**: 34-38
26. Foutz TJ, Arlow RL, McIntyre CC (2012) Theoretical principles underlying optical stimulation of a channelrhodopsin-2 positive pyramidal neuron. *Journal of Neurophysiology* **107**: 3235-3245
27. Govorunova EG, Sineshchekov OA, Janz R, Liu X, Spudich JL (2015) NEUROSCIENCE. Natural light-gated anion channels: A family of microbial rhodopsins for advanced optogenetics. *Science* **349**: 647-50
28. Malyshev AY, Roshchin MV, Smirnova GR, Dolgikh DA, Balaban PM, Ostrovsky MA (2017) Chloride conducting light activated channel GtACR2 can produce both cessation of firing and generation of action potentials in cortical neurons in response to light. *Neurosci Lett* **640**: 76-80
29. Guru A, Post RJ, Ho YY, Warden MR (2015) Making Sense of Optogenetics. *Int J Neuropsychopharmacol* **18**: pyv079
30. Berndt A, Deisseroth K (2015) OPTOGENETICS. Expanding the optogenetics toolkit. *Science* **349**: 590-1
31. Boyden ES, Zhang F, Bamberg E, Nagel G, Deisseroth K (2005) Millisecond-timescale, genetically targeted optical control of neural activity. *Nat Neurosci* **8**: 1263-1268
32. Zhang F, Wang LP, Boyden ES, Deisseroth K (2006) Channelrhodopsin-2 and optical control of excitable cells. *Nat Methods* **3**: 785-92
33. Nagel G, Szellas T, Huhn W, Kateriya S, Adeishvili N, Berthold P, Ollig D, Hegemann P, Bamberg E (2003) Channelrhodopsin-2, a directly light-gated cation-selective membrane channel. *P Natl Acad Sci USA* **100**: 13940-13945
34. Nagel G, Ollig D, Fuhrmann M, Kateriya S, Mustl AM, Bamberg E, Hegemann P (2002) Channelrhodopsin-1: A light-gated proton channel in green algae. *Science* **296**: 2395-2398
35. Mathias Mahn LG, Katayun Cohen-Kashi Malina, Pritish Patil, Yoav Printz, Shir Oring, Rivka Levy, Ilan Lampl and Ofer Yizhar (2017) High-efficiency optogenetic silencing with soma-targeted anion conducting channelrhodopsins.
36. Mohammad F, Stewart JC, Ott S, Chlebikova K, Chua JY, Koh TW, Ho J, Claridge-Chang A (2017) Optogenetic inhibition of behavior with anion channelrhodopsins. *Nat Methods* **14**: 271-274
37. Mallat MW (2014) *Human anatomy*.
38. Espeel M (2014-2015) *Embryologie en organogenese: functionele anatomie deel 1*.
39. Rand S. Swenson MD, Ph.D. (2006) *Review of Clinical and Functional Neuroscience*.
40. HEINRICHER MM (2004) *Microelectrode Recording in Movement Disorder Surgery*.
41. Oxley TJ, Opie NL, John SE, Rind GS, Ronayne SM, Wheeler TL, Judy JW, McDonald AJ, Dornom A, Lovell TJ*, et al.* (2016) Minimally invasive endovascular stent-electrode array for high-fidelity, chronic recordings of cortical neural activity. *Nat Biotechnol* **34**: 320-7
42. Mark A. Suckow SHWaCLF (2006) *The Laboratory Rat*.
43. George Paxinos CW (2007) *The rat brain in stereotaxic coordinates*.
44. Han X, Qian X, Bernstein JG, Zhou HH, Franzesi GT, Stern P, Bronson RT, Graybiel AM, Desimone R, Boyden ES (2009) Millisecond-timescale optical control of neural dynamics in the nonhuman primate brain. *Neuron* **62**: 191-8
45. Diester I, Kaufman MT, Mogri M, Pashaie R, Goo W, Yizhar O, Ramakrishnan C, Deisseroth K, Shenoy KV (2011) An optogenetic toolbox designed for primates. *Nat Neurosci* **14**: 387-97
46. Kandratavicius L, Balista PA, Lopes-Aguiar C, Ruggiero RN, Umeoka EH, Garcia-Cairasco N, Bueno LS, Leite JP (2014) Animal models of epilepsy: use and limitations. *Neuropsych Dis Treat* **10**: 1693-1705
47. Krook-Magnuson E, Armstrong C, Oijala M, Soltesz I (2013) On-demand optogenetic control of spontaneous seizures in temporal lobe epilepsy. *Nat Commun* **4**
48. Wykes RC, Heeroma JH, Mantoan L, Zheng K, MacDonald DC, Deisseroth K, Hashemi KS, Walker MC, Schorge S, Kullmann DM (2012) Optogenetic and potassium channel gene therapy in a rodent model of focal neocortical epilepsy. *Sci Transl Med* **4**: 161ra152
49. Mauss AS, Busch C, Borst A (2017) Optogenetic Neuronal Silencing in Drosophila during Visual Processing. *Sci Rep* **7**: 13823

50. Mohamed GA, Cheng RK, Ho J, Krishnan S, Mohammad F, Claridge-Chang A, Jesuthasan S (2017) Optical inhibition of larval zebrafish behaviour with anion channelrhodopsins. *BMC Biol* **15**: 103
51. Alfonsa H, Lakey JH, Lightowlers RN, Trevelyan AJ (2016) Cl-out is a novel cooperative optogenetic tool for extruding chloride from neurons. *Nat Commun* **7**: 13495
52. Raimondo JV, Kay L, Ellender TJ, Akerman CJ (2012) Optogenetic silencing strategies differ in their effects on inhibitory synaptic transmission. *Nat Neurosci* **15**: 1102-+

ADDENDUM

LIST OF ABBREVIATIONS

%	percent
‘	minutes
“	seconds
°C	degree Celcius
µm	micrometer
AAV	adeno-associated viral vector
AEDs	anti-epileptic drugs
AMPA	alpha-amino-2,3-dihydro-5-methyl-3-oxo-4-isoxazolepropanoic acid
AP	action potentials (through the thesis)
AP	anterior – posterior (surgery one: AAV injection)
Arch	archeorhodopsin
BB	blocking buffer
Ca^{2+}	calcium ion
CamKIIα	α-calcium/calmodulin-dependent kinase II
ChETA	channelrhodopsin-2 with E123T mutation
ChIEF	red-shifted channelrhodopsin variant
ChR1	channelrhodopsin-1
ChR2	channelrhodopsin-2
ChR2-H134R	channelrhodopsin-2 with H134R mutation
Cl^-	chloride ion
CNO	clozapine N-oxide
DAPI	4',6-diamidino-2-phenylindole
dH2O	distilled water
DREADD	designer receptors exclusively activated by designer drugs
DV	dorsoventral
EEG	electroencephalography
E_h	holding potential
EP	evoked potentials
eYFP	enhanced yellow fluorescent protein

g	gram
GABA	gamma-aminobutyric acid
GAD67	glutamic acid decarboxylase-67
GFP	green fluorescent protein
GtACR1	Guillardia theta anion channelrhodopsin-1
GtACR2	Guillardia theta anion channelrhodopsin-2
h	hour
H^+	proton
H_2O_2	hydrogen peroxide
Hz	hertz
K^+	potassium ion
KA	kainic acid
kg	kilogram
l	liter
LASER	Light Amplification by Stimulated Emission of Radiation
LED	light emitting diode
LFP	local field potentials
M	molar
mg	milligram
ML	mediolateral
ml	millilitre
ms	milliseconds
mV	millivolt
mW/mm^2	milliwatt/cubic millimeter = intensity
MΩ	megaohm
NA	numerical aperture
Na^+	sodium ion
$NA_2HPO_4.2H_2O$	sodium phosphate dibasic
NaCl	sodiumchloride
$NaH_2PO_4.H_20$	sodium phosphate monobasic
NeuN	neuronal nuclear antibody
ng	nanogram

nl	nanolitre
nm	nanometer
NMDA	N-methyl-D-aspartate
NpHR	halorhodopsin
PB	phosphate buffer
PBS	phosphate buffered saline
PFA	paraformaldehyde
PSP	post-synaptic potentials
RFP	red fluorescent protein
SC	subcutaneous
stGtACR2	soma-targeted Guillardia theta anion channelrhodopsin-2
SSS	superior sagittal sinus
TIF	tagged image file format
TLE	temporal lobe epilepsy
VGluT1	vesicular glutamate transporter 1 antibody
ZVI	Zeiss Vision Image

EP AMPLITUDES OF CHR2 AND GTACR2 EXPRESSING NEURONS PER PULSE DURATION

EP amplitudes (mV) were plotted against LASER output powers (mW). Graphs were made per pulse duration. These graphs show that when EP are provoked, EP amplitudes are not dependent on the depth, both with ChR2 and GtACR2 expressing neurons (figures 33, 34, 35, 36, 37, 38, 39, 40, 41 and 42).

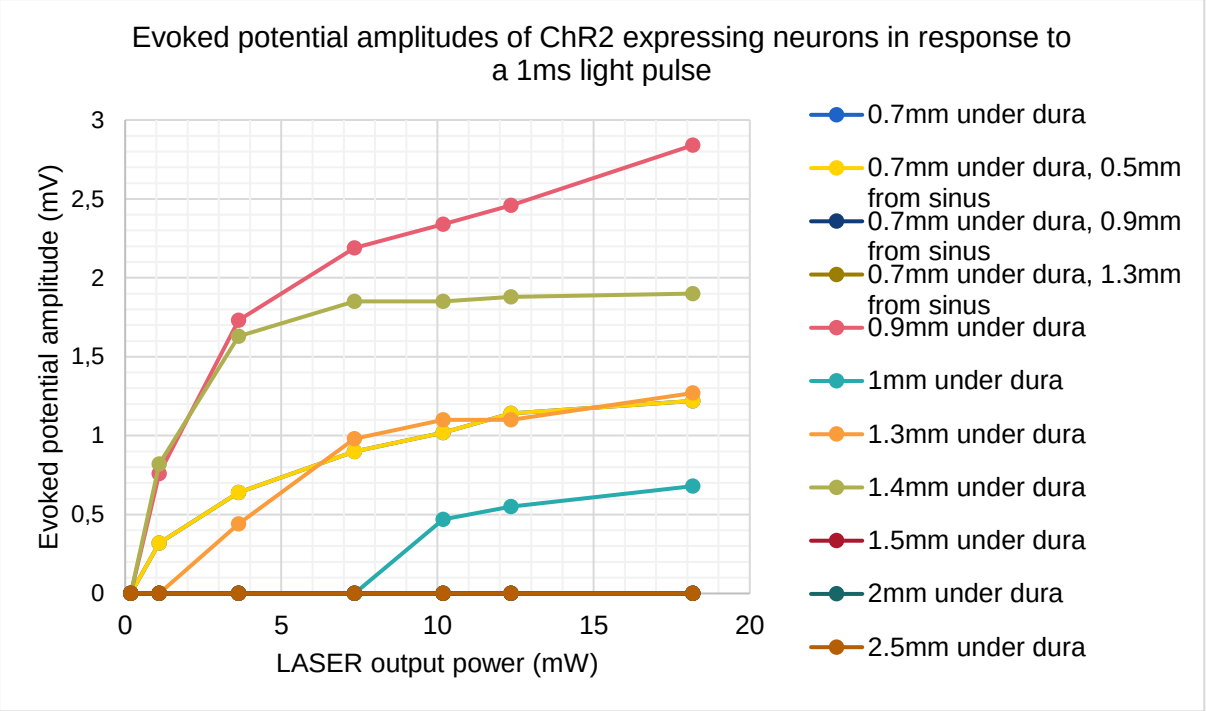

Figure 30: Evoked potential (EP) amplitudes of ChR2 expressing neurons in response to a 1ms light pulse at different depths and distances from the optic fiber tip. EP amplitudes (y-axis) are plotted against LASER output powers (x-axis).

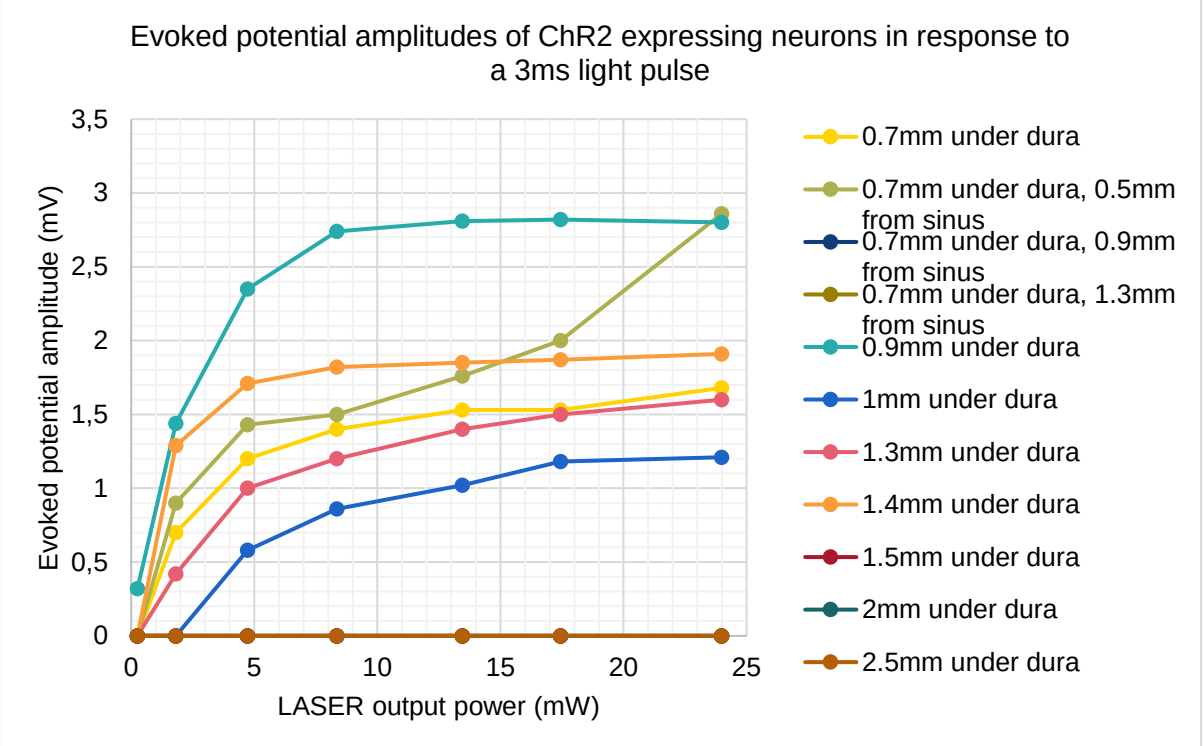

Figure 31: Evoked potential (EP) amplitudes of ChR2 expressing neurons in response to a 3ms light pulse at different depths and distances from the optic fiber tip. EP amplitudes (y-axis) are plotted against LASER output powers (x-axis).

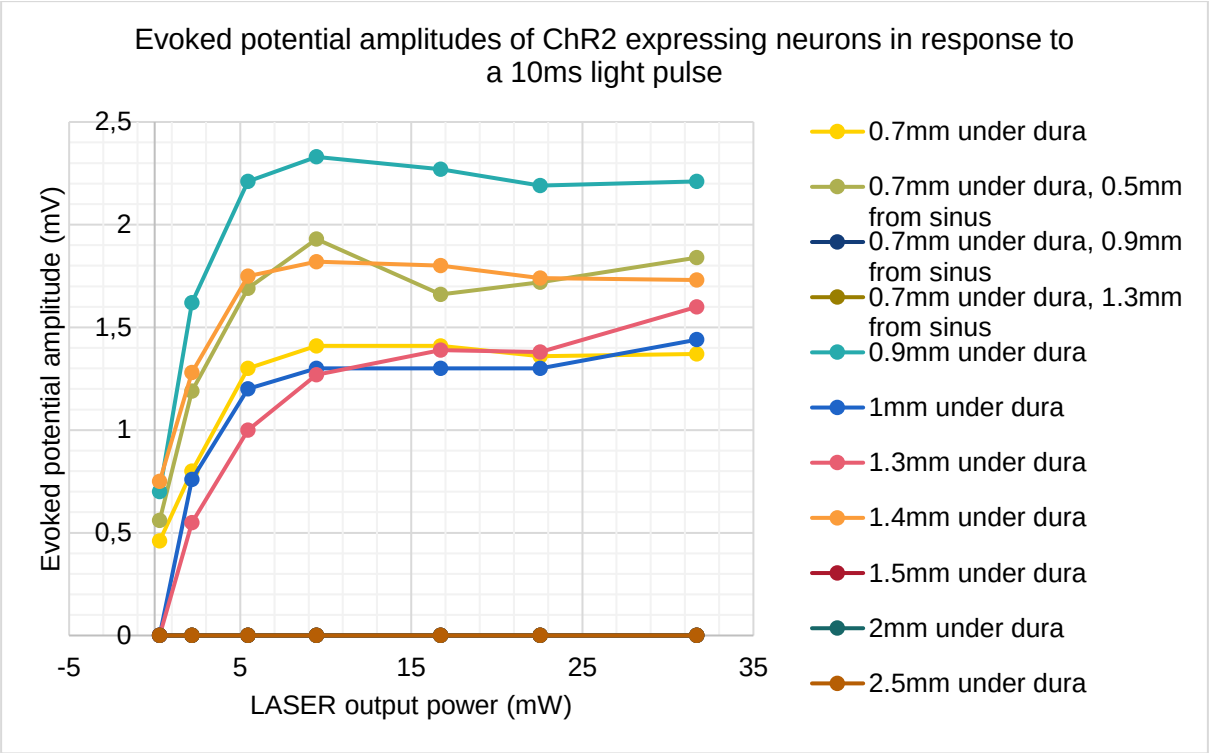

Figure 32: Evoked potential (EP) amplitudes of ChR2 expressing neurons in response to a 10ms light pulse at different depths and distances from the optic fiber tip. EP amplitudes (y-axis) are plotted against LASER output powers (x-axis).

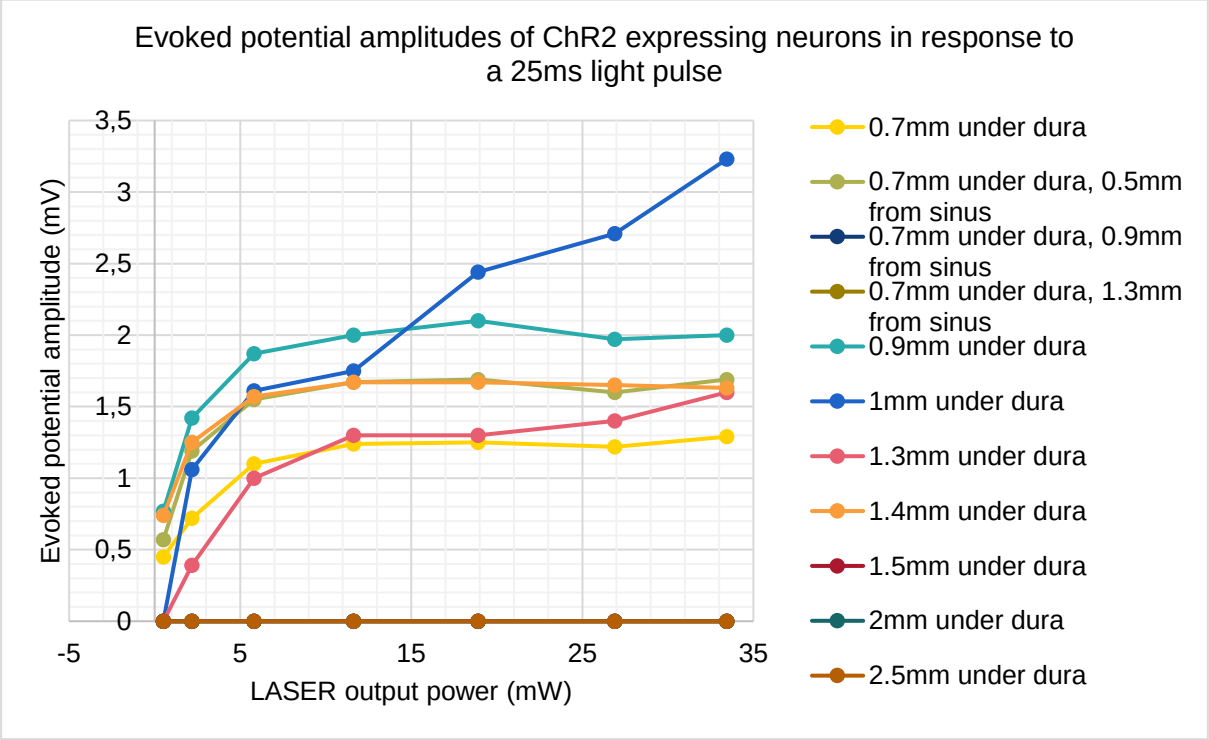

Figure 33: Evoked potential (EP) amplitudes of ChR2 expressing neurons in response to a 25ms light pulse at different depths and distances from the optic fiber tip. EP amplitudes (y-axis) are plotted against LASER output powers (x-axis).

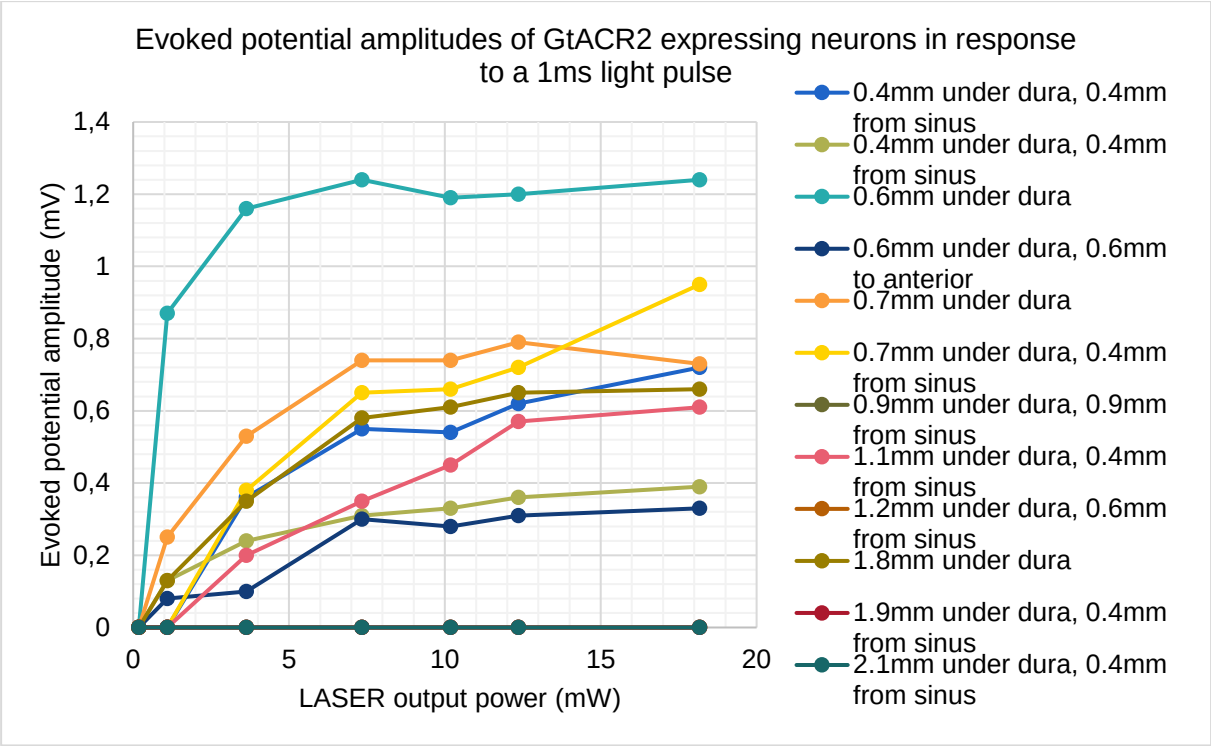

Figure 34: Evoked potential (EP) amplitudes of GtACR2 expressing neurons in response to a 1ms light pulse at different depths and distances from the optic fiber tip. EP amplitudes (y-axis) are plotted against LASER output powers (x-axis).

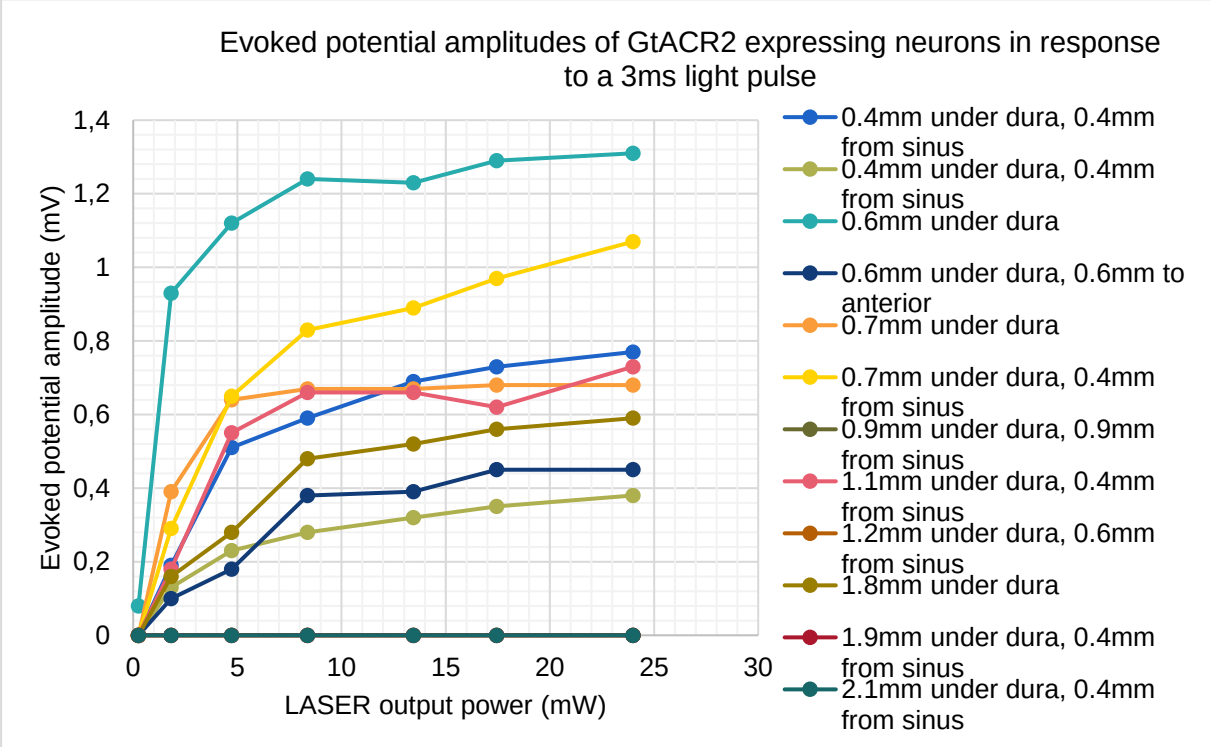

Figure 35: Evoked potential (EP) amplitudes of GtACR2 expressing neurons in response to a 3ms light pulse at different depths and distances from the optic fiber tip. EP amplitudes (y-axis) are plotted against LASER output powers (x-axis).

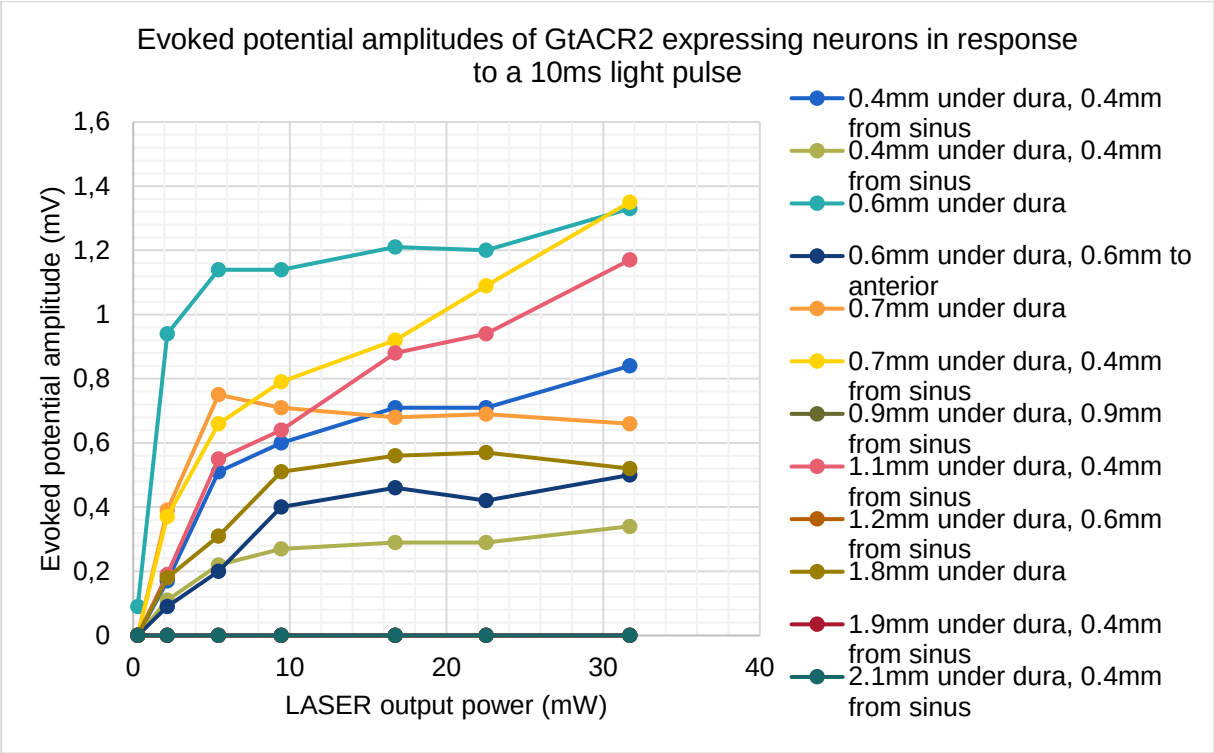

Figure 36: Evoked potential (EP) amplitudes of GtACR2 expressing neurons in response to a 10ms light pulse at different depths and distances from the optic fiber tip. EP amplitudes (y-axis) are plotted against LASER output powers (x-axis).

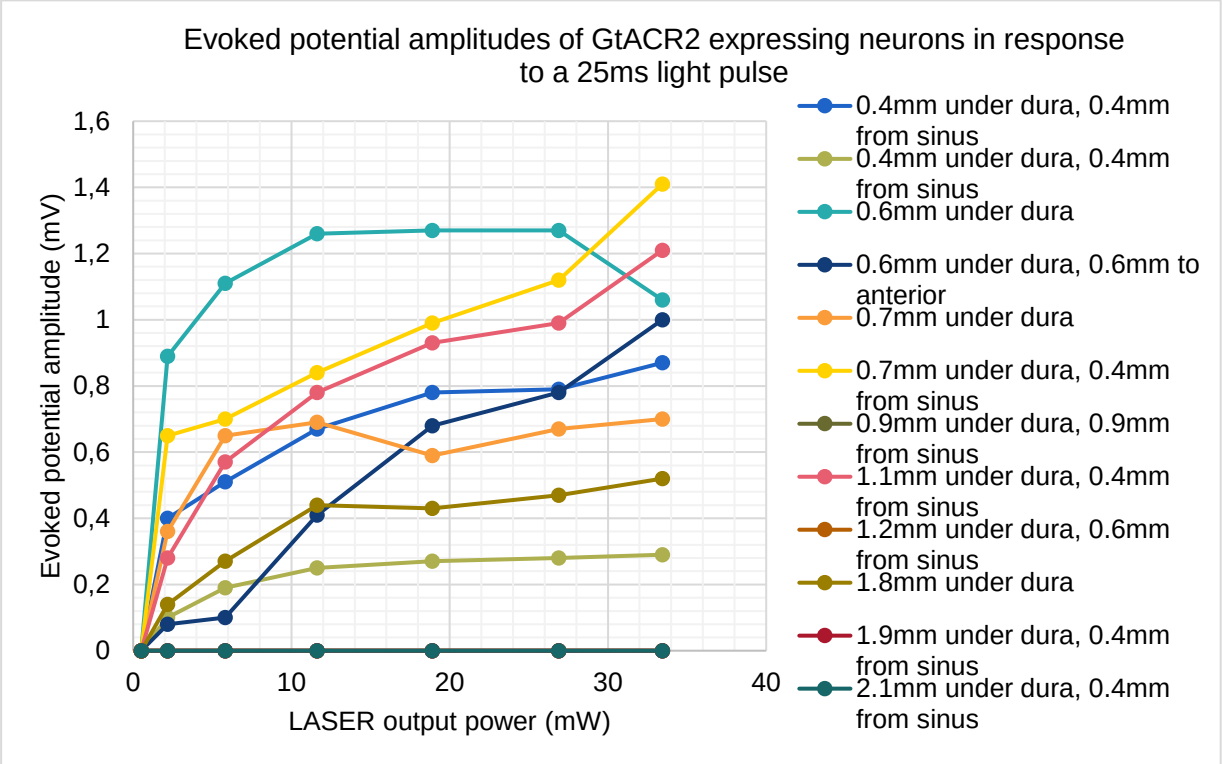

Figure 37: Evoked potential (EP) amplitudes of GtACR2 expressing neurons in response to a 25ms light pulse at different depths and distances from the optic fiber tip. EP amplitudes (y-axis) are plotted against LASER output powers (x-axis).

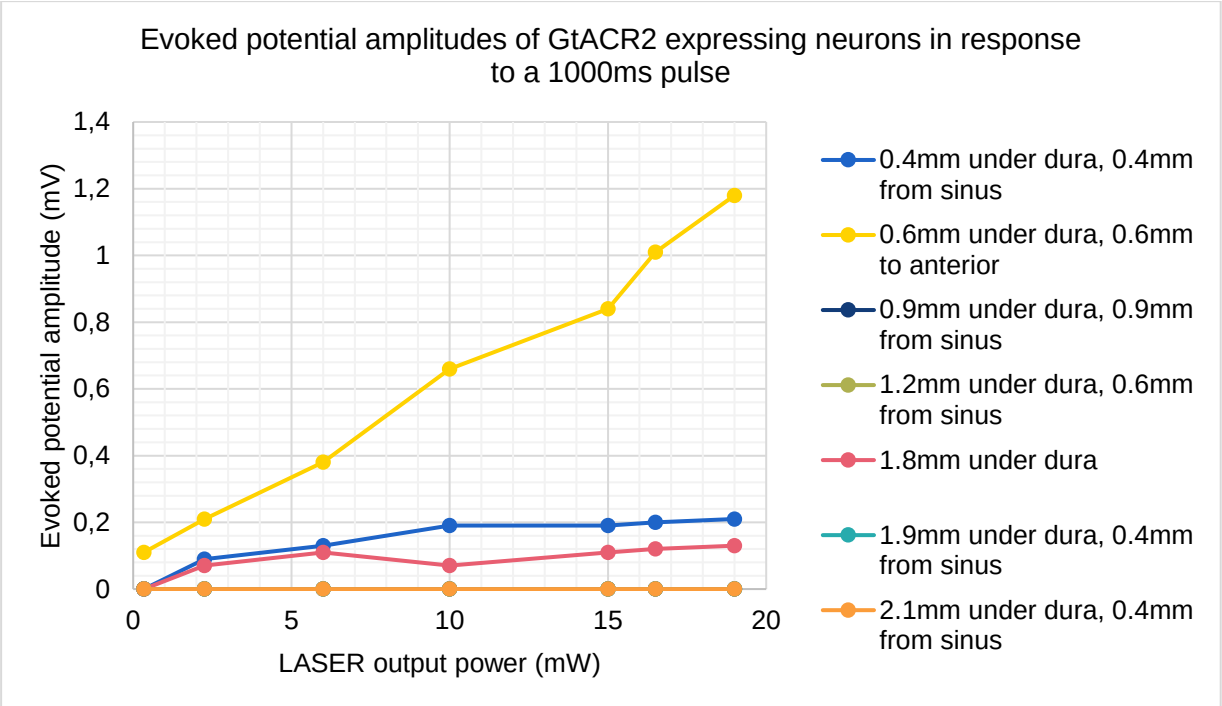

Figure 38: Evoked potential (EP) amplitudes of GtACR2 expressing neurons in response to a 1000ms light pulse at different depths and distances from the optic fiber tip. EP amplitudes (y-axis) are plotted against LASER output powers (x-axis).

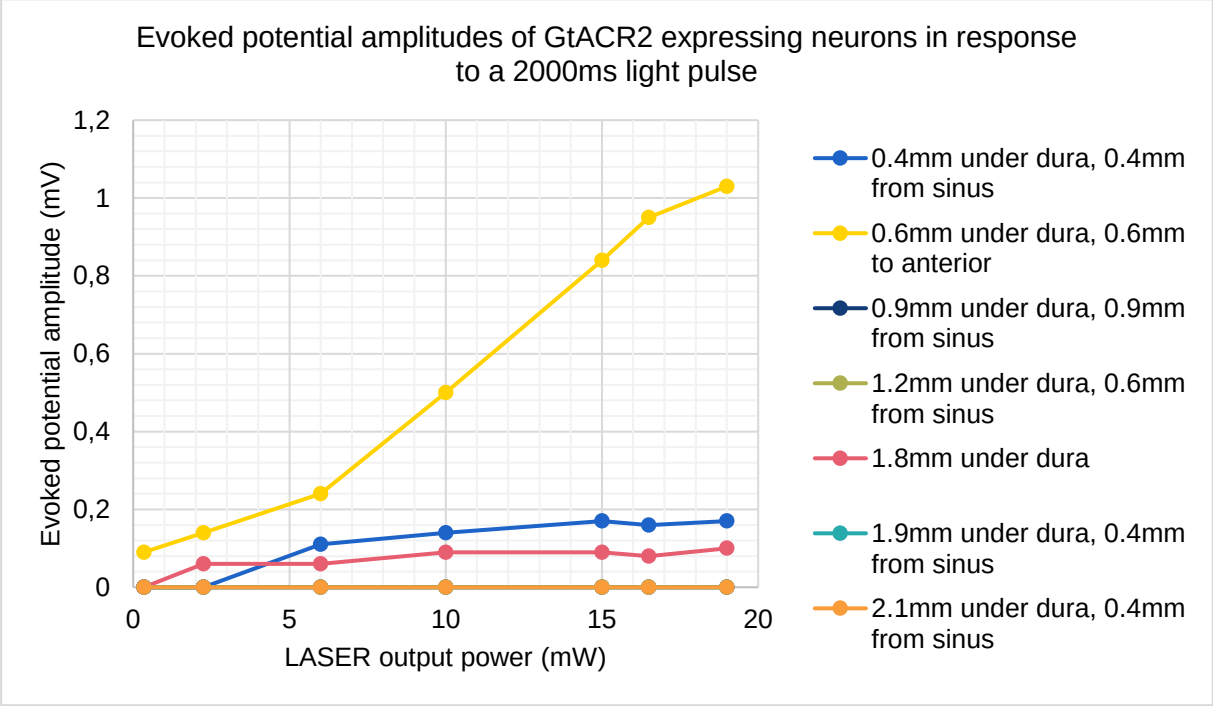

Figure 39: Evoked potential (EP) amplitudes of GtACR2 expressing neurons in response to a 2000ms light pulse at different depths and distances from the optic fiber tip. EP amplitudes (y-axis) are plotted against LASER output powers (x-axis).